ATOMIC DATA AND THEIR APPLICATIONS AND ASSESSMENT

KANTI M. AGGARWAL

Astrophysics Research Centre
Queen's University Belfast
BELFAST BT7 1NN
Northern Ireland, UK

25 October 2010

ATOMIC PARAMETERS

- ENERGY LEVELS
  $E_j - E_i = h\nu_{ij} = hc/\lambda_{ij}$

- RADIATIVE RATES (A, s^{-1}),
  OSCILLATOR STRENGTHS (f, dimensionless),
  LINE STRENGTHS (S, a.u.)

$f_{i,j} = \frac{mc}{8\pi^2 e^2}\lambda_{ji}^2 \frac{\omega_j}{\omega_i} A_{ji} = 1.49 \times 10^{-16}\ \lambda_{ij}^2(\omega_j/\omega_i)A_{ji}$

E1: $A_{ji} = \frac{2.0261\times10^{18}}{\omega_j\lambda_{ji}^3}$ S and $f_{ij} = \frac{303.75}{\lambda_{ji}\omega_i}$ S,

E2: $A_{ji} = \frac{1.1199\times10^{18}}{\omega_j\lambda_{ji}^5}$ S and $f_{ij} = \frac{167.89}{\lambda_{ji}^3\omega_i}$ S,

M1: $A_{ji} = \frac{2.6974\times10^{13}}{\omega_j\lambda_{ji}^3}$ S and $f_{ij} = \frac{4.044\times10^{-3}}{\lambda_{ji}\omega_i}$ S,

M2: $A_{ji} = \frac{1.4910\times10^{13}}{\omega_j\lambda_{ji}^5}$ S and $f_{ij} = \frac{2.236\times10^{-3}}{\lambda_{ji}^3\omega_i}$ S.

λ is in $\mathring{A}$.

- LIFE-TIME
  $\tau_j = \frac{1}{\sum_i A_{ji}}$

- COLLISION STRENGTHS (CROSS SECTIONS)
  $\Omega_{ij}(E) = {k_i}^2\omega_i\sigma_{ij}(\pi {a_0}^2)$

• EFFECTIVE COLLISION STRENGTHS (RATE COEFFICIENTS)

$\Upsilon(T_e) = \int_0^\infty \Omega e^{-E_j/kT_e} d(E_j/kT_e)$

$q_{ij} = \frac{8.63\times10^{-6}}{\omega_i {T_e}^{1/2}} e^{-E_{ij}/kT_e} \Upsilon_{ij}$ $\quad$ cm^3/s

$q_{ji} = \frac{8.63\times10^{-6}}{\omega_j {T_e}^{1/2}} \Upsilon_{ij}$ cm^3/s

• LINE INTENSITY RATIO

$\mathrm{I}_{ji} = A_{ji} N_j N_{A,Z} N_A h\nu_{ji} \frac{n}{1+N_{He}} \frac{L}{4\pi}$ $\quad$ ergs cm^{-2} s^{-1} sr^{-1}

$\mathrm{R} = \frac{I(\lambda_{ij})}{I(\lambda_{mn})} = \frac{A_{ji}}{A_{nm}} \frac{\lambda_{mn}}{\lambda_{ij}} \frac{N_j}{N_n}$

APPLICATIONS

1. Astrophysical Plasmas ($T_e \leq$ 50,000 K)

2. Solar Plasmas ($T_e \sim 10^6$ K)

3. Lasing Plasmas ($T_e \sim 10^7$ K)

4. Fusion Plasmas ($T_e \sim 10^8$ K)

PROGRAMS

Structure Codes:

CIV3, SS, AS, MBPT, MCHF, MCDF, GRASP, FAC

Scattering Codes:

R-matrix: RM, BPRM, RMPS, DARC
DW: UCL, HULLAC, FAC

PROBLEMS

1. NUMBER OF STATES/LEVELS
2. CONFIGURATION INTERACTION (CI)
3. ENERGY/TEMPERATURE RANGE
4. RELATIVISTIC EFFECTS (TCC, B-P, DIRAC)
5. NUMBER OF PARTIAL WAVES
6. TOP-UP
7. PSEUDO/SPURIOUS RESONANCES
8. PSEUDO STATES
9. RESONANCES
10. RADIATION DAMPING

Table 1. Comparison of energy levels (in Ryd) of **Ni XIX**.

Index	Configuration	Level	Expt.	GRASP	FAC1	FAC2	FAC3	CIV3	
1	$2s^22p^6$	$^1S_0$	0.00000	0.00000	0.0000	0.0000	0.0000	00.0000	
2	$2s^22p^53s$	$^3P^o_2$	64.74789	64.59266	64.6260	64.6243	64.4843	64.7487	
3	$2s^22p^53s$	$^1P^o_1$	64.90591	64.75556	64.7985	64.7975	64.6398	64.9061	
4	$2s^22p^53s$	$^3P^o_0$	66.04590	65.89549	65.9271	65.9254	65.7771	66.0446	
5	$2s^22p^53s$	$^3P^o_1$	66.14067	65.99248	66.0313	66.0302	65.8688	66.1407	
6	$2s^22p^53p$	$^3S_1$	67.26964	67.11863	67.1474	67.1432	67.0258	67.2651	
7	$2s^22p^53p$	$^3D_2$	67.52411	67.38277	67.4226	67.4217	67.2797	67.5369	
8	$2s^22p^53p$	$^3D_3$	67.72295	67.57916	67.6142	67.6126	67.4797	67.7241	
9	$2s^22p^53p$	$^1P_1$	67.79872	67.65968	67.6981	67.6972	67.5554	67.8000	
10	$2s^22p^53p$	$^3P_2$	67.96467	67.82370	67.8663	67.8659	67.7191	67.9624	
11	$2s^22p^53p$	$^3P_0$	68.48787	68.36453	68.4100	68.4089	68.2512	68.5097	
12	$2s^22p^53p$	$^3D_1$	68.77114	68.63561	68.6713	68.6701	68.5236	68.7856	
13	$2s^22p^53p$	$^3P_1$	69.10029	68.95945	68.9950	68.9937	68.8487	69.0956	
14	$2s^22p^53p$	$^1D_2$	69.14025	69.00116	69.0392	69.0383	68.8875	69.1412	
15	$2s^22p^53p$	$^1S_0$	70.08373	70.13098	70.2260	70.2142	69.9528	70.1169	
16	$2s^22p^53d$	$^3P^o_0$	71.06029	70.91200	70.9373	70.9311	70.7882	71.0476	
...									
26	$2s^22p^53d$	$^1F^o_3$	72.77962	72.64864	72.6662	72.6624	72.4993	72.7769	
27	$2s^22p^53d$	$^1P^o_1$	73.28227	73.24505	73.2607	73.2589	73.0681	73.3565	
28	$2s2p^63s$	$^3S_1$	76.16370	75.91019	75.9615	75.9601	75.8236	74.8222⋆	
29	$2s2p^63s$	$^1S_0$	76.69223	76.45810	76.5362	76.5328	76.3398	75.3098⋆	
30	$2s2p^63p$	$^3P^o_0$		78.62091	78.6761	78.6750	78.5453	77.2530⋆	
31	$2s2p^63p$	$^3P^o_1$	78.56398	78.66211	78.7185	78.7176	78.5857	77.2996⋆	
32	$2s2p^63p$	$^3P^o_2$		78.91529	78.9692	78.9679	78.8400	77.5506⋆	
33	$2s2p^63p$	$^1P^o_1$	78.97314	79.06836	79.1314	79.1314	78.9879	77.6960⋆	
34	$2s2p^63d$	$^3D_1$		82.35964	82.3940	82.3854	82.2644	80.8726⋆	
35	$2s2p^63d$	$^3D_2$		82.37523	82.4097	82.4011	82.2800	80.8917⋆	
36	$2s2p^63d$	$^3D_3$		82.40539	82.4397	82.4311	82.3103	80.9221⋆	
37	$2s2p^63d$	$^1D_2$		82.82932	82.8588	82.8563	82.7004	81.3372⋆	$\Delta E \sim 1.5$ Ryd

Expt.: NIST data from `http://www.physics.nist.gov/PhysRefData`
GRASP: Present GRASP results for 89 levels
FAC1: Present FAC results for 89 levels
FAC2: Present FAC results for 157 levels
FAC3: Present FAC results for 3601 levels
CIV3: Hibbert et al. (1993)

Reference: Aggarwal & Keenan, A&A 460 (2006) 959

Table 5. Target levels of **Ni XVII** (in Ryd).

Index	Configuration	Level	Expt.	CIV3(a)	CIV3(b)	GRASP	FAC	MCHF	CIV3(c)
1	$3s^2$	$^1S_0$	0.0000	0.0000	0.0000	0.0000	0.0000	0.0012	0.0000
2	3s3p	$^3P^o_0$	2.4097	2.4215	2.4105	2.4017	2.4031	2.4080	2.4097
3		$^3P^o_1$	2.4844	2.4908	2.4851	2.4769	2.4781	2.4844	2.4842
4		$^3P^o_2$	2.6763	2.6631	2.6775	2.6672	2.6682	2.6795	2.6767
5		$^1P^o_1$	3.6569	3.6921	3.6577	3.7032	3.6991	3.6571	3.6563
6	$3p^2$	$^3P_0$	5.7220	5.7743	5.7236	5.7489	5.7477	5.7179	5.7212
7		$^1D_2$	5.8213	5.8420	5.8194	5.8313	5.8299	5.8319	5.8073
8		$^3P_1$	5.8668	5.9006	5.8677	5.8907	5.8896	5.8648	5.8671
9		$^3P_2$	6.1013	6.1074	6.0981	6.1198	6.1183	6.1052	6.0949
10		$^1S_0$	6.8756	6.9137	6.8776	6.9419	6.9354	6.8905	6.8773
...									
38	3s4p	$^3P^o_0$		21.1846	21.1854	21.1393	21.1447	21.1653	23.1620⋆
39		$^3P^o_1$	21.2640	21.1891	21.3130	21.1458	21.1505	21.1725	23.1762⋆
40		$^3P^o_2$		21.2729	21.2740	21.2404	21.2453	21.2789	23.2439⋆
41		$^1P^o_1$	21.2635	21.2756	21.2271	21.2468	21.2500	21.2712	21.5875
...									
54	3p4p	$^1P_1$		24.0147	24.0158	23.9494	23.9501	23.9622	26.0314⋆
55		$^3D_1$		24.1739	24.1749	24.1247	24.1273	24.1436	25.8978⋆
56		$^3D_2$		24.1911	24.1922	24.1416	24.1432	24.1641	26.0162⋆
57		$^3P_0$		24.2223	24.2231	24.1704	24.1838	24.1854	26.0511⋆
58		$^3P_1$		24.3348	24.3357	24.2975	24.3062	24.3216	26.2009⋆
59		$^3D_3$		24.3790	24.3801	24.3498	24.3494	24.3826	26.2151⋆
60		$^3P_2$		24.4151	24.4159	24.3834	24.3948	24.4056	26.3343⋆
61		$^3S_1$		24.4556	24.4567	24.4230	24.4245	24.4500	26.2929⋆
62		$^1D_2$		24.6015	24.6019	24.5860	24.5988	24.5837	26.2320⋆
63		$^1S_0$		24.9082	24.9091	24.9123	24.9292	24.8707	26.5520⋆
...									
...									$\Delta E \sim 2$ Ryd

Expt.: NIST data from `http://physics.nist.gov/PhysRefData`
CIV3(a): Present *ab initio* energies from the CIV3 code [20]
CIV3(b): Present *adjusted* energies from the CIV3 code [20]
GRASP: Present energies from the GRASP [22] code
FAC: Present energies from the FAC [23] code
MCHF: Calculations of Fawcett [17] for the lowest 26 levels, and of Tachiev and Froese-Fischer [18] for higher levels
CIV3(c): Calculations of Das et al. [19] from the CIV3 code [20]

TABLE I. Comparison of energies of the $(3p^3)\ ^2D^o_{3/2,\ 5/2}$ and the $[3s3p(^3P^o)3d]\ ^2D^o_{3/2,\ 5/2}$ levels relative to the ground state (in cm^{-1}) for Ar VI, Ti X, Fe XIV, and Ni XVI.

Ion	Conf.	Level	Expt.	CIV3	GRASP	MBPT	Other Calculations
Ar VI	$3p^3$	$^2D^o_{3/2}$	260 067[a]	258 792	258 725	328 864	263 818[d]
		$^2D^o_{5/2}$	260 271[a]	258 999	258 927	328 820	264 049[d]
	$3s3p(^3P^o)3d$	$^2D^o_{3/2}$	328 990[a]	328 546	332 210	259 555	329 393[d]
		$^2D^o_{5/2}$	328 959[a]	328 503	332 173	259 765	329 376[d]
Ti X	$3p^3$	$^2D^o_{3/2}$	413 405[b] 413 397[c]	411 783	412 906	518 071	413 696[c] 420 140[d]
		$^2D^o_{5/2}$	414 353[b] 414 365[c]	412 744	413 816	518 144	414 767[c] 421 231[d]
	$3s3p(^3P^o)3d$	$^2D^o_{3/2}$	519 045[b] 519 034[c]	518 132	523 208	412 733	518 693[c] 519 638[d]
		$^2D^o_{5/2}$	519 112[b] 519 113[c]	518 179	523 257	413 695	518 759[c] 519 794[d]
Fe XIV	$3p^3$	$^2D^o_{3/2}$	576 388[b] 576 383[c]	574 390	576 560	716 538	577 008,[c] 585 036,[d] 574 348[e]
		$^2D^o_{5/2}$	580 273[b] 580 233[c]	578 250	580 109	717 163	581 116,[c] 589 811,[d] 577 607[e]
	$3s3p(^3P^o)3d$	$^2D^o_{3/2}$	717 253[b] 717 195[c]	716 442	721 986	576 065	717 135,[c] 717 636,[d] 721 576[e]
		$^2D^o_{5/2}$	717 865[b] 717 861[c]	717 165	722 513	579 912	717 829,[c] 718 479[d] 722 122[e]
Ni XVI	$3p^3$	$^2D^o_{3/2}$	662 678[c]	660 535	663 336	821 780	663 637,[c] 671 692,[d] 664 776[f]
		$^2D^o_{5/2}$	669 946[c]	667 692	669 956	822 910	671 262,[c] 680 721,[d] 670 212[f]
	$3s3p(^3P^o)3d$	$^2D^o_{3/2}$	822 364[c]	821 739	827 336	662 532	822 587,[c] 822 328,[d] 838 659[f]
		$^2D^o_{5/2}$	823 538[c]	823 061	828 329	669 745	823 884,[c] 823 823,[d] 839 047[f]

[a]Experimental results of Raineri *et al.* [6].
[b]Experimental results of Redfors and Litzen [7].
[c]Experimental and theoretical results of Churilov and Levashov [8].
CIV3: Calculation of Gupta and Msezane [9] (For Ar VI and Ti X: Present results).
GRASP: Calculation of Aggarwal *et al.* [10] (For Ar VI, Ti X and Fe XIV: Present results).
MBPT: Relativistic many-body perturbation theory calculation of Safronova *et al.* [1].
[d]Calculation of Fawcett [11].
[e]Calculation of Froese Fischer and Liu [12].
[f]Calculation of Bhatia and Doschek [13].

TABLE II. Eigenvector composition of the $(3p^3)\ ^2D^o$ and the $[3s3p(^3P^o)3d]\ ^2D^o$ levels (corresponding to our CIV3 calculations) in Ar VI, Ti X, Fe XIV, and Ni XVI.

Ar VI	$3p^3\ (^2D^o_{3/2})$	$-0.7830\ 3p^3\ (^2D^o_{3/2}) - 0.4481\ 3s3p(^3P^o)3d(^2D^o_{3/2})$
	$3s3p(^3P^o)3d(^2D^o_{3/2})$	$0.6554\ 3s3p(^3P^o)3d(^2D^o_{3/2}) - 0.6103\ 3p^3\ (^2D^o_{3/2})$
	$3p^3\ (^2D^o_{5/2})$	$-0.7844\ 3p^3\ (^2D^o_{5/2}) - 0.4462\ 3s3p(^3P^o)3d(^2D^o_{5/2})$
	$3s3p(^3P^o)3d(^2D^o_{5/2})$	$0.6542\ 3s3p(^3P^o)3d(^2D^o_{5/2}) - 0.6099\ 3p^3\ (^2D^o_{5/2})$
Ti X	$3p^3\ (^2D^o_{3/2})$	$-0.8068\ 3p^3\ (^2D^o_{3/2}) - 0.4165\ 3s3p(^3P^o)3d(^2D^o_{3/2})$
	$3s3p(^3P^o)3d(^2D^o_{3/2})$	$-0.6838\ 3s3p(^3P^o)3d(^2D^o_{3/2}) + 0.5703\ 3p^3\ (^2D^o_{3/2})$
	$3p^3\ (^2D^o_{5/2})$	$0.8126\ 3p^3\ (^2D^o_{5/2}) - 0.4103\ 3s3p(^3P^o)3d(^2D^o_{5/2})$
	$3s3p(^3P^o)3d(^2D^o_{5/2})$	$-0.6772\ 3s3p(^3P^o)3d(^2D^o_{5/2}) - 0.5723\ 3p^3\ (^2D^o_{5/2})$
Fe XIV	$3p^3\ (^2D^o_{3/2})$	$-0.7935\ 3p^3\ (^2D^o_{3/2}) + 0.4105\ 3s3p(^3P^o)3d(^2D^o_{3/2})$
	$3s3p(^3P^o)3d(^2D^o_{3/2})$	$0.6892\ 3s3p(^3P^o)3d(^2D^o_{3/2}) + 0.5420\ 3p^3\ (^2D^o_{3/2})$
	$3p^3\ (^2D^o_{5/2})$	$0.8198\ 3p^3\ (^2D^o_{5/2}) + 0.3971\ 3s3p(^3P^o)3d(^2D^o_{5/2})$
	$3s3p(^3P^o)3d(^2D^o_{5/2})$	$0.6718\ 3s3p(^3P^o)3d(^2D^o_{5/2}) - 0.5617\ 3p^3\ (^2D^o_{5/2})$
Ni XVI	$3p^3\ (^2D^o_{3/2})$	$0.7684\ 3p^3\ (^2D^o_{3/2}) - 0.4126\ 3s3p(^3P^o)3d(^2D^o_{3/2})$
	$3s3p(^3P^o)3d(^2D^o_{3/2})$	$-0.6892\ 3s3p(^3P^o)3d(^2D^o_{3/2}) - 0.5193\ 3p^3\ (^2D^o_{3/2})$
	$3p^3\ (^2D^o_{5/2})$	$-0.8200\ 3p^3\ (^2D^o_{5/2}) - 0.3888\ 3s3p(^3P^o)3d(^2D^o_{5/2})$
	$3s3p(^3P^o)3d(^2D^o_{5/2})$	$0.6555\ 3s3p(^3P^o)3d(^2D^o_{5/2}) + 0.5606\ 3p^3\ (^2D^o_{5/2})$

A.Z.M. is supported by Division of Chemical Sciences, Office of Basic Energy Sciences, Office of Energy Research, United States Department of Energy.

[1] U. I. Safronova, C. Namba, J. R. Albritton, W. R. Johnson, and M. S. Safronova, Phys. Rev. A **65**, 022507 (2002).
[2] D. W. Savin, in *Spectroscopic Challenges of Photoionized Plasmas*, edited by G. Ferland and D. W. Savin, ASP Conf. Series 247 (ASP, San Francisco, 2001), p. 399.
[3] D. J. Hillier, and T. Lanz, in *Spectroscopic Challenges of Photoionized Plasmas* (Ref. [2]), p. 343.
[4] A. Hibbert, Comput. Phys. Commun. **9**, 141 (1975).
[5] K. G. Dyall, I. P. Grant, C. T. Johnson, F. A. Parpia, and E. P. Plummer, Comput. Phys. Commun. **55**, 424 (1989).
[6] M. Raineri *et al.*, Phys. Scr. **45**, 584 (1992).
[7] A. Redfors and U. Litzen, J. Opt. Soc. Am. B **6**, 1447 (1989).
[8] S. S. Churilov and V. E. Levashov, Phys. Scr. **48**, 425 (1993).
[9] G. P. Gupta and A. Z. Msezane, J. Phys. B **34**, 4217 (2001).
[10] K. M. Aggarwal, F. P. Keenan, and A. Z. Msezane, At. Data Nucl. Data Tables **85**, 453 (2003).
[11] B. C. Fawcett, At. Data Nucl. Data Tables **28**, 557 (1983).
[12] C. Froese Fischer and B. Liu, At. Data Nucl. Data Tables **34**, 261 (1986).
[13] A. K. Bhatia and G. A. Doschek, At. Data Nucl. Data Tables **71**, 69 (1999).
[14] U. I. Safronova, W. R. Johnson, and H. G. Berry, Phys. Rev. A **61**, 052503 (2000)
[15] C. Froese Fischer (personal website: http://atoms.vuse.vanderbilt.edu/Elements/Ni/Al_28.14.mcdhf-lev.it.db).
[16] R. Das, N. C. Deb, K. Roy, and A. Z. Msezane, Phys. Scr. **67**, 401 (2003)

Table 1. Energy levels (in Ryd) and mixing coefficients of **Fe XVI**.

Index	Configuration	Level	NIST	GRASP[a]	GRASP[b]	FAC[c]	Mixing coefficients[d]
1	$2p^6 3s$	$^2S_{1/2}$	0.00000	0.00000	0.00000	0.00000	0.999(1)
2	$2p^6 3p$	$^2P^o_{1/2}$	2.52598	2.56393	2.56618	2.54757	0.999(2)
3	$2p^6 3p$	$^2P^o_{3/2}$	2.71688	2.75844	2.75486	2.73706	0.999(3)
4	$2p^6 3d$	$^2D_{3/2}$	6.15562	6.20499	6.19591	6.16949	0.999(4)
5	$2p^6 3d$	$^2D_{5/2}$	6.18209	6.23332	6.22081	6.19510	0.999(5)
6	$2p^5 3s^2$	$^2P^o_{3/2}$	52.60745	52.36353	52.31794	52.41746	0.985(6)
7	$2p^5 3s^2$	$^2P^o_{1/2}$	53.51871	53.30895	53.24028	53.33762	0.985(7)
8	$2p^5 3s3p$	$^4S_{3/2}$		54.13058	54.08374	54.17709	-0.886(8), 0.431(14)
9	$2p^5 3s3p$	$^4D_{5/2}$	54.51199	54.37708	54.32940	54.42538	0.828(9), -0.416(13)
10	$2p^5 3s3p$	$^4D_{7/2}$		54.43349	54.38145	54.47626	0.998(10)
11	$2p^5 3s(^1P)3p$	$^2D_{3/2}$	54.79442	54.43554	54.38938	54.48851	0.676(17), 0.536(11)⋆
12	$2p^5 3s(^1P)3p$	$^2P_{1/2}$	54.68514	54.56418	54.52045	54.61812	0.582(12), -0.541(16), 0.478(18)
13	$2p^5 3s3p$	$^4P_{5/2}$		54.67382	54.62489	54.72388	0.810(13), 0.481(21)
14	$2p^5 3s3p$	$^4P_{3/2}$	55.55084	54.67609	54.62869	54.72922	0.543(11), 0.507(14), 0.431(22)⋆
15	$2p^5 3s(^1P)3p$	$^2S_{1/2}$	55.05876	54.89407	54.84442	54.93897	0.646(15), -0.537(18)
16	$2p^5 3s3p$	$^4D_{1/2}$	55.35947	55.28057	55.21306	55.30909	0.797(16), 0.453(12)
17	$2p^5 3s3p$	$^4D_{3/2}$	55.48705	55.37720	55.30739	55.40431	0.696(17), -0.430(11)
18	$2p^5 3s3p$	$^4P_{1/2}$	55.48705	55.39547	55.33684	55.42765	0.648(18), 0.545(15)
19	$2p^5 3s(^3P)3p$	$^2D_{5/2}$	54.79442	55.49867	55.44467	55.52949	-0.908(19)
20	$2p^5 3s(^3P)3p$	$^2P_{3/2}$	55.85156	55.50353	55.43583	55.52862	0.663(14), -0.521(20)⋆
21	$2p^5 3s(^1P)3p$	$^2D_{5/2}$	55.67842	55.57474	55.50469	55.60006	-0.788(21), 0.464(9),
22	$2p^5 3s(^1P)3p$	$^2P_{3/2}$		55.63602	55.58697	55.67262	-0.642(22), 0.561(20), -0.418(24)
23	$2p^5 3s(^3P)3p$	$^2P_{1/2}$		56.31892	56.25643	56.34105	0.737(23), -0.420(12), -0.419(15)
24	$2p^5 3s(^3P)3p$	$^2D_{3/2}$	56.65347	56.48207	56.40948	56.48980	0.761(24), -0.412(11)
25	$2p^5 3s(^3P)3p$	$^2S_{1/2}$	57.10911	57.04715	56.99370	57.07898	0.894(25)
26	$2p^5 3p^2$	$^4P^o_{3/2}$		57.11374	57.06488	57.15728	-0.579(26), 0.471(30)
27	$2p^5 3p^2(^1D)$	$^2P^o_{1/2}$		57.11721	57.06704	57.16091	0.708(27), -0.447(63)
28	$2p^5 3p^2$	$^4P^o_{5/2}$		57.18875	57.13944	57.22878	0.861(28), -0.457(35)
29	$2p^5 3p^2$	$^2F^o_{7/2}$		57.20144	57.14806	57.24572	-0.828(29)
30	$2p^5 3p^2(^1D)$	$^2P^o_{3/2}$		57.27558	57.22768	57.32069	-0.517(26), -0.415(30)⋆
31	$2p^5 3p^2(^1D)$	$^2D^o_{5/2}$		57.40167	57.35118	57.44791	-0.624(31), 0.442(42)
32	$2p^5 3p^2(^3P)$	$^2D^o_{3/2}$		57.43847	57.39127	57.48571	0.783(32), 0.420(43)
33	$2p^5 3p^2$	$^4P^o_{1/2}$		57.45866	57.40547	57.49659	-0.765(33), 0.490(45)
34	$2p^5 3p^2$	$^4D^o_{7/2}$		57.47691	57.42105	57.51299	0.944(34)
35	$2p^5 3p^2$	$^4D^o_{5/2}$		57.49089	57.43729	57.53061	0.591(51), 0.555(35), 0.404(28)⋆
36	$2p^5 3p^2$	$^4D^o_{1/2}$		57.93073	57.87458	57.96637	0.788(36), -0.440(45)
37	$2p^5 3p^2(^1D)$	$^2D^o_{3/2}$		57.97229	57.91773	58.01218	0.617(48), -0.465(37)⋆
...							
41	$2p^5 3s3d$	$^4P^o_{5/2}$	58.25730	58.17918	58.11794	58.22565	0.799(41), -0.449(59)
42	$2p^5 3p^2$	$^2F^o_{5/2}$		58.19900	58.12751	58.21310	-0.641(42), -0.442(31)
43	$2p^5 3p^2$	$^4D^o_{3/2}$		58.21215	58.14156	58.23244	0.655(43), -0.410(37)
44	$2p^5 3s3d$	$^4F^o_{7/2}$		58.21941	58.16102	58.25588	0.885(44)
45	$2p^5 3p^2$	$^2S^o_{1/2}$		58.28129	58.21189	58.30146	0.712(45), 0.538(33), 0.447(36)

NIST: `http://physics.nist.gov/PhysRefData`
a: Coulomb energies
b: QED corrected energies
c: Energies from the Flexible Atomic Code of Gu (2003)
d: Mixing coefficient of the level (in bracket)

Reference: Aggarwal & Keenan, A&A 463 (2007) 399

Table 1a. Energy levels (in Ryd) of **Kr XXXII** and their lifetimes (τ). $a{\pm}b \equiv a{\times}10^{\pm b}$.

Index	Configuration	Level	NIST	GRASP[a]	GRASP[b]	FAC[c]	FAC[d]	τ (s)
1	$2s^2 2p$	$^2P^o_{1/2}$	0.00000	0.00000	0.00000	0.00000	0.00000	...
2	$2s^2 2p$	$^2P^o_{3/2}$	4.48854	4.58493	4.48151	4.48186	4.48198	9.445-07
3	$2s2p^2$	$^4P_{1/2}$	6.36064	6.35072	6.35647	6.36803	6.37143	8.238-10
4	$2s2p^2$	$^4P_{3/2}$		9.29024	9.21194	9.22372	9.22956	9.249-09
5	$2s2p^2$	$^4P_{5/2}$	10.51857	10.68049	10.51277	10.52220	10.52539	1.100-09
6	$2s2p^2$	$^2D_{3/2}$	13.02611	13.21325	13.09327	13.09731	13.09155	2.035-11
7	$2s2p^2$	$^2P_{1/2}$	18.49362⋆	13.84111	13.79048	13.79100	13.78281	9.761-12
8	$2s2p^2$	$^2D_{5/2}$	15.27859	15.45618	15.25149	15.25688	15.25573	6.903-11
9	$2s2p^2$	$^2S_{1/2}$	13.69543⋆	18.69851	18.56711	18.56632	18.56000	1.161-11
10	$2s2p^2$	$^2P_{3/2}$	18.58374	18.87320	18.67950	18.67822	18.66902	7.580-12

NIST: `http://physics.nist.gov/PhysRefData`
a: Coulomb energies
b: QED corrected energies
c: Energies from the Flexible Atomic Code (FAC) of Gu (2003) for 125 level calculations
d: Energies from FAC for 528 level calculations

Table 1b. Level designations of **Kr XXXII** and their mixing coefficients in LSJ and jj coupling.

				Mixing Coefficients	
Index	Configuration	LSJ	$jj^{a,b,c}$	jj	LSJ[d]
1	$2s^2 2p$	$^2P^o_{1/2}$	2p−1(1)1	0.994	0.994(1)
2	$2s^2 2p$	$^2P^o_{3/2}$	2p+1(3)3	0.990	0.990(2)
3	$2s2p^2$	$^4P_{1/2}$	2s+1(1)1	0.913	0.905(3)
4	$2s2p^2$	$^4P_{3/2}$	2s+1(1)1 2p−1(1)0 2p+1(3)3	0.809	-0.985(4)
5	$2s2p^2$	$^4P_{5/2}$	2s+1(1)1 2p−1(1)2 2p+1(3)5	0.930	0.837(5), -0.546(8)
6	$2s2p^2$	$^2D_{3/2}$	2s+1(1)1 2p−1(1)2 2p+1(3)3	0.772	0.905(6), 0.416(10)
7	$2s2p^2$	$^2P_{1/2}$	2s+1(1)1 2p−1(1)2 2p+1(3)1	0.896	0.852(7)⋆
8	$2s2p^2$	$^2D_{5/2}$	2s+1(1)1 2p+2(4)5	0.930	0.837(8), 0.546(5)
9	$2s2p^2$	$^2S_{1/2}$	2s+1(1)1 2p+2(0)1	0.963	0.839(9), -0.485(7)⋆
10	$2s2p^2$	$^2P_{3/2}$	2s+1(1)1 2p+2(4)3	0.955	0.903(10), -0.401(6)

Reference: Aggarwal et al., ADNDT 94 (2008) 323

Table 1a. Energy levels (in Ryd) of **Kr XXXI** and their lifetimes (τ). $a\pm b \equiv a\times 10^{\pm b}$.

Index	Configuration	Level	NIST	GRASP[a]	GRASP[b]	FAC[c]	FAC[d]	τ (s)
1	$2s^2 2p^2$	$^3P_0$	0.00000	0.00000	0.00000	0.00000	0.00000	...
2	$2s^2 2p^2$	$^3P_1$	3.61609	3.69492	3.60398	3.60578	3.60354	1.144-06
3	$2s^2 2p^2$	$^1D_2$		4.52135	4.36446	4.36441	4.36194	2.413-04
4	$2s^2 2p^2$	$^3P_2$	4.35768⋆	8.73022	8.51380	8.51474	8.51210	4.996-07
5	$2s^2 2p^2$	$^1S_0$		10.42485	10.27283	10.26871	10.27511	2.300-07
6	$2s2p^3$	$^5S^o_2$		10.82914	10.67291	10.68447	10.69184	5.797-10
7	$2s2p^3$	$^3D^o_1$	13.94421	14.11946	14.01161	14.01472	14.01308	1.569-11
8	$2s2p^3$	$^3D^o_2$	15.07053	15.26290	15.09115	15.09677	15.09803	4.246-11
9	$2s2p^3$	$^3D^o_3$	16.25245	16.57749	16.29281	16.29740	16.29637	5.481-11
10	$2s2p^3$	$^3P^o_0$	17.82347	18.00803	17.86023	17.86094	17.86471	1.461-11
11	$2s2p^3$	$^3P^o_1$	18.21714	18.47128	18.28221	18.28365	18.28331	1.048-11
12	$2s2p^3$	$^1D^o_2$		19.12984	18.88301	18.88392	18.87998	9.784-12
13	$2s2p^3$	$^3S^o_1$	19.60956	19.88707	19.71085	19.70806	19.70206	5.100-12
14	$2s2p^3$	$^3P^o_2$	18.79853⋆	22.50478	22.22767	22.22648	22.22245	9.607-12
15	$2s2p^3$	$^1P^o_1$		24.89853	24.63150	24.62681	24.62072	4.369-12

NIST: `http://physics.nist.gov/PhysRefData`
a: Coulomb energies
b: QED corrected energies
c: Energies from the Flexible Atomic Code (FAC) of Gu (2003) for 236 level calculations
d: Energies from FAC for 564 level calculations

Table 1b. Level designations of **Kr XXXI** and their mixing coefficients in LSJ and jj coupling.

				Mixing Coefficients	
Index	Configuration	LSJ	jj[a,b,c]	jj	LSJ[d]
1	$2s^2 2p^2$	$^3P_0$	2p−2(0)0	0.986	0.886(1), 0.455(5)
2	$2s^2 2p^2$	$^3P_1$	2p−1(1)1 2p+1(3)2	0.997	0.997(2)
3	$2s^2 2p^2$	$^1D_2$	2p−1(1)1 2p+1(3)4	0.984	-0.712(3), 0.697(4)⋆
4	$2s^2 2p^2$	$^3P_2$	2p+2(4)4	0.981	0.710(4), 0.696(3)⋆
5	$2s^2 2p^2$	$^1S_0$	2p+2(0)0	0.980	0.875(5), -0.459(1)
6	$2s2p^3$	$^5S^o_2$	2s+1(1)1 2p+1(3)4	0.849	0.856(6), 0.463(14)
7	$2s2p^3$	$^3D^o_1$	2s+1(1)1 2p+1(3)2	0.918	0.759(7), -0.492(11)
8	$2s2p^3$	$^3D^o_2$	2s+1(1)1 2p−1(1)0 2p+2(4)4	0.796	-0.792(8), -0.430(6), 0.404(14)
9	$2s2p^3$	$^3D^o_3$	2s+1(1)1 2p−1(1)2 2p+2(4)6	1.000	1.000(9)
10	$2s2p^3$	$^3P^o_0$	2s+1(1)1 2p−1(1)0 2p+2(0)0	1.000	-1.000(10)
11	$2s2p^3$	$^3P^o_1$	2s+1(1)1 2p−1(1)2 2p+2(4)2	0.675	-0.714(11), -0.546(7), 0.418(13)
12	$2s2p^3$	$^1D^o_2$	2s+1(1)1 2p−1(1)2 2p+2(4)4	0.675	0.670(12), -0.507(8), -0.495(14)⋆
13	$2s2p^3$	$^3S^o_1$	2s+1(1)1 2p−1(1)2 2p+2(0)2	0.675	0.691(13), 0.537(15), 0.447(11)
14	$2s2p^3$	$^3P^o_2$	2s+1(1)1 2p+3(3)4	0.870	0.718(12), 0.615(14)⋆
15	$2s2p^3$	$^1P^o_1$	2s+1(1)1 2p+3(3)2	0.938	0.761(15), -0.530(13)

Reference: Aggarwal et al., ADNDT 94 (2008) 323

Table 5. Comparison of oscillator strengths for some transitions of **Ni XIX**. ($a\pm b \equiv a\times10^{\pm b}$).

Transition		GRASP1	GRASP2	FAC	CIV3
1	3	1.300-1	1.2931-1	1.252-1	1.254-1
1	5	9.927-2	9.8688-2	9.382-2	9.420-2
1	17	1.025-2	1.0273-2	9.979-3	1.130-2
1	23	8.188-1	8.1883-1	8.201-1	7.986-1
1	27	2.457-0	2.4206-0	2.287-0	2.300-0
1	31	4.709-2	4.6852-2	4.876-2	4.250-2
1	33	2.898-1	2.8881-1	2.894-1	2.767-1
2	6	4.957-2	4.9457-2	4.967-2	4.854-2
2	7	4.855-2	4.8515-2	4.733-2	4.742-2
2	8	1.548-1	1.5469-1	1.531-1	1.522-1
2	9	1.873-3	1.8944-3	1.662-3	1.940-3
2	10	6.557-2	6.5560-2	6.481-2	6.476-2
2	13	3.868-3	3.8913-3	3.587-3	3.940-3
2	28	6.660-2	6.6925-2	6.192-2	5.336-2
3	6	1.500-3	1.5137-3	1.415-3	1.567-3
3	7	8.620-2	8.6214-2	8.591-2	8.580-2
3	9	1.038-1	1.0380-1	1.026-1	1.015-1
3	10	9.025-2	9.0265-2	8.797-2	8.757-2
3	11	3.395-2	3.4100-2	3.356-2	3.440-2
3	15	2.360-2	2.3411-2	2.247-2	2.157-2
3	28	2.867-2	2.8813-2	2.641-2	2.310-2⋆
3	29	2.568-2	2.5681-2	2.409-2	1.890-2⋆
4	6	1.157-3	1.1556-3	1.216-3	1.200-3
4	12	1.130-1	1.1288-1	1.103-1	1.109-1
4	13	2.082-1	2.0805-1	2.069-1	2.048-1
4	28	6.083-2	6.1118-2	5.653-2	4.950-2⋆
5	10	7.700-4	7.7368-4	7.448-4	7.333-4
5	11	8.211-3	8.1051-3	7.902-3	7.500-3
5	12	5.982-2	5.9843-2	5.948-2	5.920-1
5	13	3.826-2	3.8248-2	3.743-2	3.707-2
5	14	1.867-1	1.8663-1	1.841-1	1.833-1
5	15	4.149-2	4.1547-2	4.034-2	4.073-2
5	28	3.397-2	3.4138-2	3.184-2	2.757-2⋆
5	29	1.645-2	1.6461-2	1.513-2	1.177-2⋆

Differences are up to 50%

GRASP1: Present calculations from the GRASP code with 89 levels
GRASP2: Present calculations from the GRASP code with 157 levels
FAC: Present calculations from the FAC code with 3601 levels
CIV3: Calculations of Hibbert et al. (1993) from the CIV3 code

Reference: Aggarwal & Keenan, A&A 460 (2006) 959

Table 5. Comparison of oscillator strengths for some transitions of **Fe IX**. ($a\pm b \equiv a\times10^{\pm b}$).

Transition		GRASP1	GRASP2		FAC	CIV3		SS
i	j	f_L	f_L	f_L/f_V	f_L	f_L	f_L/f_V	f_L
1	3	3.608-4	3.698-4	9.5-1	3.746-4	3.376-4	4.7-1	3.050-4
1	10	5.350-3	5.527-3	9.4-1	5.735-3	5.555-3	6.1-1	5.140-3
1	13	2.998-0	3.147-0	9.6-1	3.054-0	2.983-0	9.8-1	2.950-0
2	14	6.976-2	6.950-2	1.2-0	6.551-2	5.293-2⋆	1.1-0	7.230-2
3	14	2.153-2	2.144-2	1.2-0	2.035-2	1.619-2⋆	1.1-0	2.260-2
3	15	4.894-2	4.871-2	1.2-0	4.586-2	3.753-2⋆	1.1-0	5.020-2
3	17	1.642-4	1.550-4	1.1-0	1.655-4	1.775-6⋆	1.2+1	1.970-4
4	14	1.379-3	1.373-3	1.2-0	1.314-3	1.025-3⋆	1.1-0	1.510-3
4	15	1.498-2	1.489-2	1.2-0	1.419-2	1.140-2⋆	1.1-0	1.570-2
4	16	5.547-2	5.507-2	1.2-0	5.201-2	4.268-2⋆	1.1-0	5.650-2
4	17	3.387-4	3.559-4	7.9-1	3.651-4	1.440-4⋆	8.4-1	4.260-4
5	16	3.840-2	4.070-2	6.8-1	3.831-2	2.371-2⋆	6.1-1	4.090-2
6	15	3.589-2	3.790-2	6.9-1	3.565-2	2.210-2⋆	6.1-1	3.840-2
6	16	1.343-3	1.479-3	4.6-1	1.379-3	6.951-4⋆	3.9-1	1.360-3
6	17	3.911-4	4.026-4	1.0-0	3.814-4	7.108-4⋆	9.7-1	3.890-4
7	14	3.409-2	3.593-2	6.9-1	3.386-2	2.117-2⋆	5.9-1	3.650-2
7	15	2.131-3	2.321-3	4.9-1	2.166-3	1.138-3⋆	4.1-1	2.090-3
7	16	1.110-5	8.542-6	4.1-0		1.916-5⋆	2.1+1	2.570-5
7	17	1.013-3	1.116-3	6.2-1	1.102-3	7.124-4⋆	6.8-1	1.300-3
8	15	2.227-3	2.196-3	1.1-0	2.178-3	1.662-3⋆	8.6-1	2.160-3
8	16	2.427-2	2.472-2	1.0-0	2.297-2	1.485-2⋆	8.4-1	2.500-2
8	17	8.285-3	8.070-3	8.8-1	8.398-3	5.958-3⋆	7.7-1	8.400-3
9	14	3.396-9	4.099-6	1.7+1		5.293-5⋆	1.2-1	7.600-5
9	15	1.319-2	1.301-2	9.5-1	1.292-2	6.294-3⋆	7.1-1	1.320-2
9	16	2.233-3	2.127-3	1.0-0	2.171-3	8.601-4⋆	7.9-1	1.950-3
9	17	1.517-2	1.677-2	6.1-1	1.653-2	9.927-3⋆	5.5-1	1.670-2
10	14	2.498-2	2.491-2	1.0-0	2.423-2	1.525-2⋆	7.7-1	2.520-2
10	15	1.277-2	1.273-2	1.1-0	1.229-2	8.574-3⋆	7.7-1	1.370-2
10	17	4.187-5	4.433-5	6.4-1	5.209-5	9.070-6⋆	1.0-0	5.260-5
11	14	2.672-3	2.654-3	1.1-0	2.590-3	1.616-3⋆	8.3-1	2.620-3
11	15	1.310-2	1.335-2	1.0-0	1.263-2	9.687-3⋆	7.6-1	1.390-2
11	16	8.752-3	8.828-3	1.1-0	8.385-3	6.936-3⋆	7.6-1	1.020-2
11	17	9.782-3	1.019-2	6.4-1	1.056-2	3.555-3⋆	5.2-1	9.540-3
12	15	2.086-7	1.974-6	2.8+1		1.581-5⋆	6.1-2	9.850-6
12	16	1.252-2	1.202-2	9.8-1	1.265-2	8.283-3⋆	7.0-1	1.300-2
12	17	1.699-2	1.773-2	8.5-1	1.614-2	1.111-2⋆	7.0-1	1.760-2
13	14	1.346-5	1.332-5	9.4-1		9.250-6⋆	1.3-1	1.730-5
13	15	1.021-4	1.013-4	7.1-1	1.079-4	2.409-5⋆	2.3-1	1.290-4
13	17	6.538-3	7.049-3	3.0-1	7.333-3	1.635-3⋆	1.5-1	7.330-3

GRASP1: Present calculations from the GRASP code with 1099 levels
GRASP2: Present calculations from the GRASP code with 2471 levels
FAC: Present calculations from the FAC code with 1219 levels
CIV3: Calculations of Verma et al. (2006) from the CIV3 code
SS: Calculations of Stroey et al. (2002) from the SuperStructure code

Table 3. Comparison of radiative rates (A-values, s^{-1}) for transitions among the lowest 40 levels of Ti X. $a\pm b \equiv a\times 10^{\pm b}$.

I	J	f (GRASP4) n≤6	GRASP1 n≤3	GRASP2 n≤4	GRASP3 n≤5	GRASP4 n≤6	FAC n≤6	CIV3	NIST
1	6	7.6−02	1.1+09	1.1+09	1.2+09	1.1+09	1.1+09	9.0+08	1.1+08
1	8	1.5−01	7.1+09	7.2+09	7.2+09	7.2+09	7.2+09	3.1+09	6.9+09
1	9	2.6−01	1.4+10	1.4+10	1.5+10	1.5+10	1.4+10	1.8+10	1.3+10
2	6	3.5−03	9.4+07	9.9+07	1.0+08	9.9+07	9.8+07	1.6+08	9.5+07
2	8	3.5−02	2.9+09	3.2+09	3.2+09	3.2+09	3.1+09	5.7+09	2.7+09
2	9	1.2−01	1.2+10	1.2+10	1.2+10	1.2+10	1.2+10	8.3+09	1.2+10
3	24	2.8−01	2.3+10	2.3+10	2.3+10	2.2+10	2.2+10	3.1+09	7.6+09
3	25	9.0−02	7.4+09	7.1+09	7.3+09	7.3+09	7.1+09	2.7+10	2.3+10
4	24	1.3−02	2.0+09	2.0+09	2.1+09	2.1+09	2.0+09	1.5+09	1.8+10
4	25	1.2−01	1.9+10	1.9+10	1.9+10	1.9+10	1.9+10	5.2+09	1.6+09
4	27	2.2−01	1.2+10	1.2+10	1.2+10	1.2+10	1.2+10	2.2+10	1.1+10
6	37	5.8−04	1.9+08	1.4+08	1.3+08	1.3+08	1.4+08	3.3+08	1.9+08
7	13	8.4−03	3.6+08	3.4+08	3.4+08	3.4+08	3.5+08	1.9+08	3.7+08
7	36	1.4−02	1.4+09	1.4+09	1.4+09	1.4+09	1.4+09	1.5+08*	1.3+09
8	17	1.2−02	3.8+08	3.3+08	3.2+08	3.1+08	3.3+08	7.0+08	3.9+08
8	34	2.6−01	1.7+10	1.9+10	1.9+10	1.9+10	1.9+10	2.7+10	1.6+10
9	17	6.8−02	1.5+09	1.5+09	1.5+09	1.5+09	1.5+09	1.1+09	1.1+09
9	33	2.5−02	1.2+09	9.1+08	8.3+08	8.2+08	8.3+08	2.1+09	1.1+09
10	37	5.1−02	6.7+09	7.4+09	7.6+09	7.6+09	7.4+09	7.1+09	5.5+09
11	31	5.4−02	1.0+09	9.7+08	9.6+08	9.6+08	9.6+08	1.0+10*	1.1+09
11	40	1.8−02	5.6+08	6.2+08	6.3+08	6.4+08	6.3+08	8.5+08	5.4+08
12	33	6.2−08	9.7+07	4.5+06	3.0+04	3.9+03	0.0+00	2.0+07	8.2+07

GRASP and FAC : present calculations from the GRASP and FAC codes
CIV3: Singh et al [ADNDT 96 (2010) 759
NIST: http://physics.nist.gov/

Does adjustment of energy levels (fine-tuning) improves the accuracy of A (and Ω) values?

Fig. 4. Comparison of collision strengths for some transitions of Fe XVI. Continuous curve: present results, broken curve: Cornille et al. (1997), circles: 6-16, triangles: 6-17, and stars: 7-15 transition.

Figure 12. Comparison of effective collision strengths for some transitions of Fe XVI.

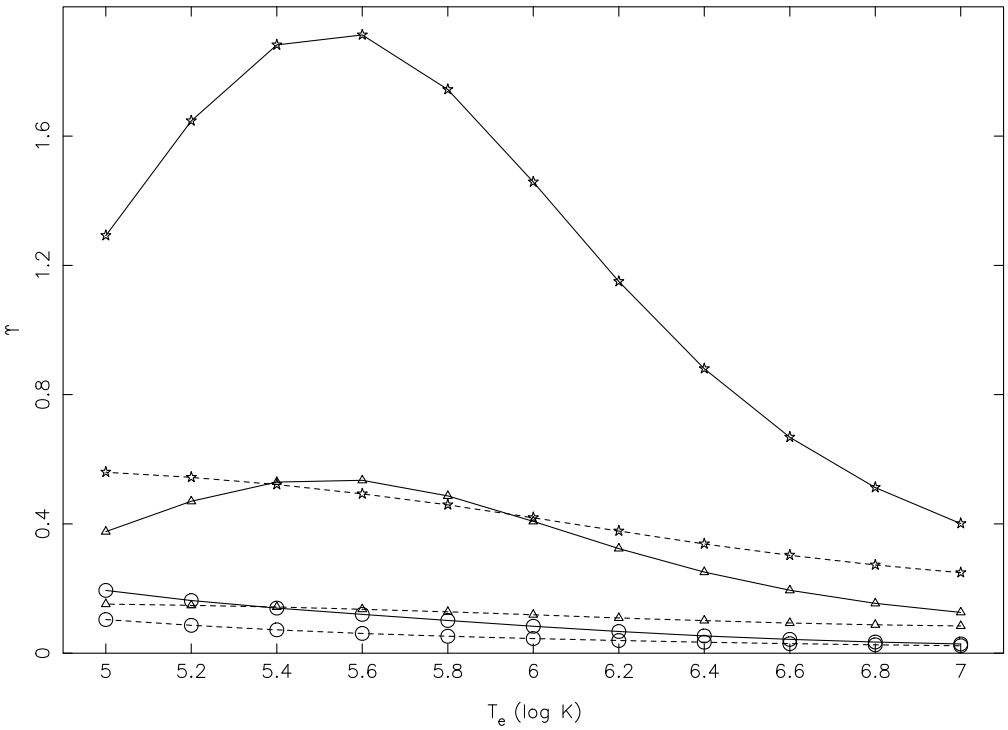

Fig. 12. Comparison of effective collision strengths for some transitions of Fe XVI. Continuous curve: present results, broken curve: Eissner et al. (1999), circles: 4-10, triangles: 9-12, and stars: 11-12 transition.

Table 2. Comparison of effective collision strengths (Υ) for some resonance transitions from ground state to higher excited levels of **Fe XVI**. $a-b \equiv a\times10^{-b}$.

Index	Configuration	Level	Present results		Bautista (2000)	
	Temperature		10^5	10^6	10^5	10^6 K
6	$2p^5 3s^2$	$^2P^o_{3/2}$	2.447−1	9.155−2	4.31−2	1.90−2
7	$2p^5 3s^2$	$^2P^o_{1/2}$	1.037−1	3.459−2	2.15−2	9.45−3
8	$2p^5 3s3p$	$^4S_{3/2}$	5.148−2	1.861−2	1.30−2	4.85−3
9	$2p^5 3s3p$	$^4D_{5/2}$	4.904−2	1.596−2	1.05−2	3.91−3
10	$2p^5 3s3p$	$^4D_{7/2}$	4.693−2	1.926−2	9.96−3	3.71−3
11	$2p^5 3s(^1P)3p$	$^2D_{3/2}$	3.649−2	1.577−2	7.62−3	3.31−3
12	$2p^5 3s(^1P)3p$	$^2P_{1/2}$	1.613−2	5.611−3	3.43−3	1.45−3
13	$2p^5 3s3p$	$^4P_{5/2}$	4.352−2	1.753−2	1.34−2	4.67−3
14	$2p^5 3s3p$	$^4P_{3/2}$	4.326−2	1.249−2	9.10−3	4.10−3
15	$2p^5 3s(^1P)3p$	$^2S_{1/2}$	5.151−2	1.525−2	1.35−2	5.28−3
16	$2p^5 3s3p$	$^4D_{1/2}$	2.070−2	6.464−3	4.74−3	2.22−3
17	$2p^5 3s3p$	$^4D_{3/2}$	4.261−2	1.389−2	7.93−3	3.52−3
18	$2p^5 3s3p$	$^4P_{1/2}$	2.459−2	7.970−3	1.20−2	6.25−3
19	$2p^5 3s(^3P)3p$	$^2D_{5/2}$	7.099−2	2.032−2	6.11−3	4.48−3
22	$2p^5 3s(^1P)3p$	$^2P_{3/2}$	6.313−2	1.587−2	8.32−3	3.58−3
23	$2p^5 3s(^3P)3p$	$^2P_{1/2}$	5.466−2	2.960−2	1.10−2	7.10−3
24	$2p^5 3s(^3P)3p$	$^2D_{3/2}$	7.605−2	1.482−2	1.32−2	4.93−3
25	$2p^5 3s(^3P)3p$	$^2S_{1/2}$	9.329−2	8.462−2	8.16−2	3.08−2
26	$2p^5 3p^2$	$^4P^o_{3/2}$	8.209−3	2.675−3	1.96−3	5.82−4
27	$2p^5 3p^2(^1D)$	$^2P^o_{1/2}$	4.752−3	2.387−3	1.75−3	5.59−4
28	$2p^5 3p^2$	$^4P^o_{5/2}$	6.177−3	1.311−3	9.13−4	1.93−4
29	$2p^5 3p^2$	$^2F^o_{7/2}$	6.409−3	2.533−3	2.13−3	5.76−4
30	$2p^5 3p^2(^1D)$	$^2P^o_{3/2}$	6.728−3	2.483−3	2.64−3	6.63−4
33	$2p^5 3p^2$	$^4P^o_{1/2}$	2.570−3	8.844−4	5.95−4	1.72−4
34	$2p^5 3p^2$	$^4D^o_{7/2}$	6.076−3	1.363−3	8.30−4	1.85−4
35	$2p^5 3p^2$	$^4D^o_{5/2}$	6.943−3	1.497−3	1.50−3	3.49−4
36	$2p^5 3p^2$	$^4D^o_{1/2}$	2.579−3	9.225−4	2.73−4	1.24−4
37	$2p^5 3p^2(^1D)$	$^2D^o_{3/2}$	4.327−3	1.306−3	1.36−3	2.81−4
38	$2p^5 3s3d$	$^4P^o_{1/2}$	6.293−3	4.599−3	5.26−5	1.04−5
39	$2p^5 3s3d$	$^4P^o_{3/2}$	1.259−2	8.907−3	1.21−3	3.34−4
41	$2p^5 3s3d$	$^4P^o_{5/2}$	1.436−2	9.798−3	2.40−3	7.66−4
42	$2p^5 3p^2$	$^2F^o_{5/2}$	6.331−3	2.612−3	2.27−3	5.48−4
46	$2p^5 3s3d$	$^4F^o_{5/2}$	9.051−3	5.393−3	6.68−4	1.36−4
58	$2p^5 3s3d$	$^4F^o_{3/2}$	6.779−3	4.376−3	1.75−3	4.16−4

Differences are of over an order of magnitude

Reference: Aggarwal & Keenan, J. Phys. B 41 (2008) 015701

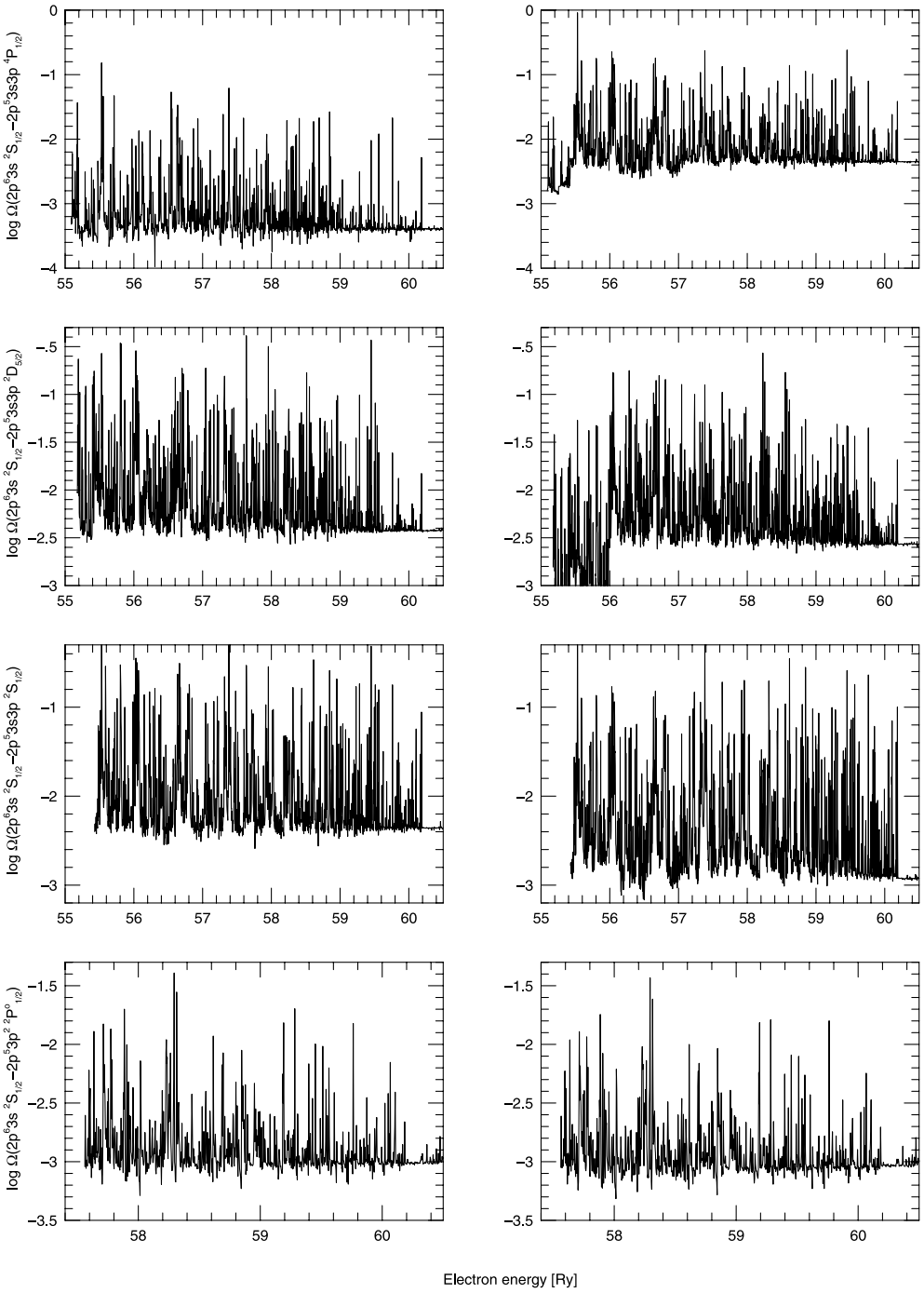

Figure 3. Comparison between collision strengths calculated with (right-hand panels) and without (left-hand panels) TCC.

3.2. Non-relativistic collision strengths

Figure 2 shows sample collision strengths for collisional excitation from the ground state to doubly excited levels of Fe XVI. The full circles represent the single-energy distorted-wave

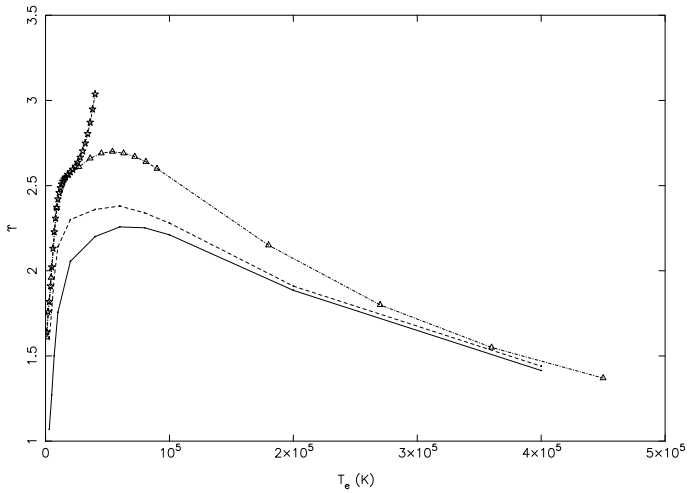

Fig. 12. Comparison of present (continuous curve) effective collision strengths with those of Blum & Pradhan (1992: dot-dash curve with stars), Zhang et al. (1994: dot-dash curve with triangles), and Tayal (2006: broken curve) for the 1−2 ($2s^2 2p\ ^2P^\circ_{1/2}$−$2s^2 2p\ ^2P^\circ_{3/2}$) transition of O IV.

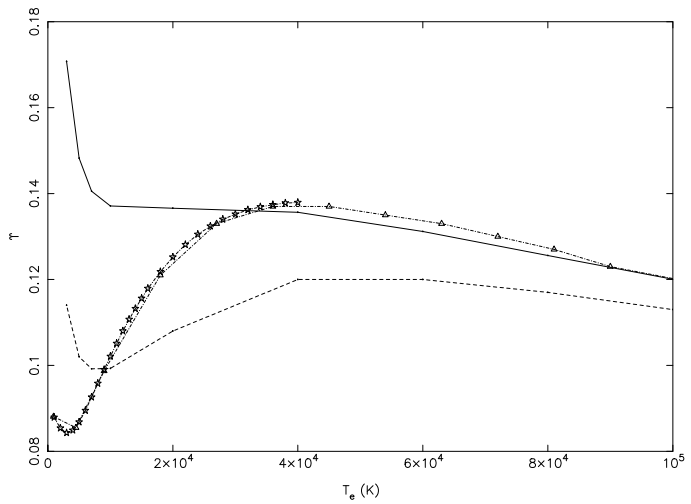

Fig. 13. Comparison of present (continuous curve) effective collision strengths with those of Blum & Pradhan (1992: dot-dash curve with stars), Zhang et al. (1994: dot-dash curve with triangles), and Tayal (2006: broken curve) for the 2−3 ($2s^2 2p\ ^2P^\circ_{3/2}$−$2s2p^2\ ^4P_{1/2}$) transition of O IV.

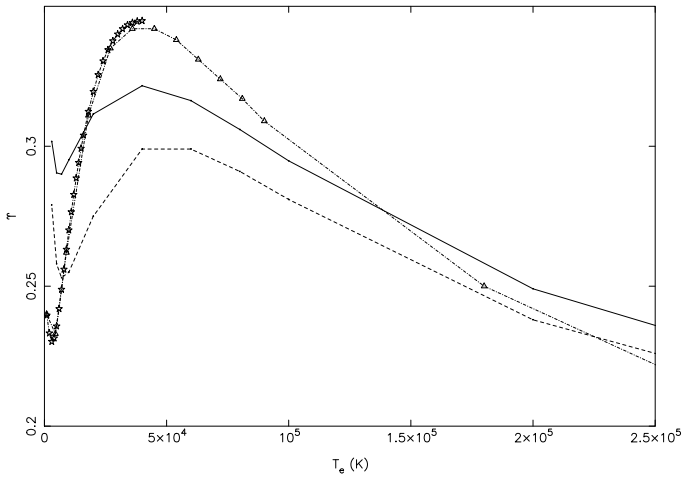

Fig. 14. Comparison of present (continuous curve) effective collision strengths with those of Blum & Pradhan (1992: dot-dash curve with stars), Zhang et al. (1994: dot-dash curve with triangles), and Tayal (2006: broken curve) for the 2−4 ($2s^2 2p\ ^2P^\circ_{3/2}$−$2s2p^2\ ^4P_{3/2}$) transition of O IV.

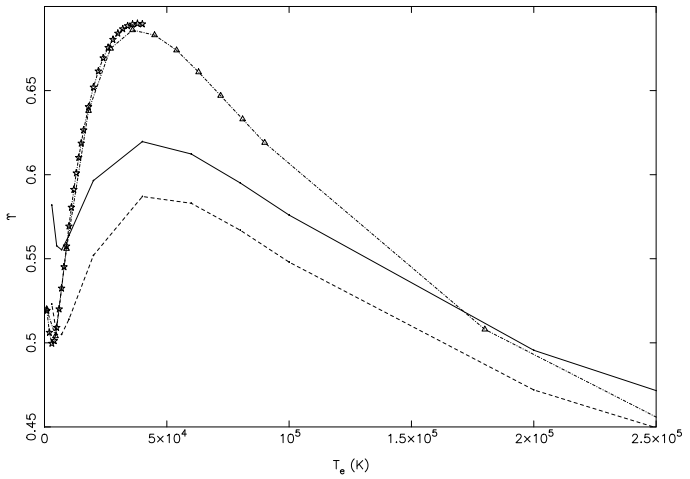

Fig. 15. Comparison of present (continuous curve) effective collision strengths with those of Blum & Pradhan (1992: dot-dash curve with stars), Zhang et al. (1994: dot-dash curve with triangles), and Tayal (2006: broken curve) for the 2−5 ($2s^2 2p\ ^2P^\circ_{3/2}$−$2s2p^2\ ^4P_{5/2}$) transition of O IV.

Differences between our values of Υ and those of Tayal (2006) are also mainly at lower temperatures, as seen in Figs. 12−17. However, the discrepancy at lower temperatures for some transitions is not only in magnitude but also in behaviour, see for example, the 2−6 transition in Fig. 16. The most likely reason for these differences in magnitude as well as behaviour is the presence (or absence) of resonances close to the threshold, as seen in Figs. 8−10. A slight shift in their placement can affect the values of Υ at lower temperatures, as also observed earlier for transitions in Fe XI (Aggarwal & Keenan 2003) and Fe XIII (Aggarwal & Keenan 2005). For example, for the 2−6 transition (not shown) we have several resonances lying close to the threshold energy. An exercise performed by removing the threshold resonances brings the two sets of Υ values into good agreement. However, for some other transitions, particularly the allowed ones, such as 2−3, 2−4 and 2−5 shown in Figs. 13−15, respectively, Tayal's values of Υ are underestimated in the entire temperature range. Since Tayal has not published his values of Ω for these transitions, it is difficult to understand the differences. Furthermore, the f-values for these transitions are very small ($<10^{-7}$), as seen in Table 3. Therefore, the differences in the Υ values could be due to the differences in the f-values and subsequently the Ω values. However, there are some transitions, such as 1−19 ($2s^2 2p\ ^2P^\circ_{1/2}$−$2s^2 3d\ ^2D_{3/2}$) and 2−20 ($2s^2 2p\ ^2P^\circ_{3/2}$−$2s^2 3d\ ^2D_{5/2}$), for which the f-values in our calculations and those of Tayal are comparable, as shown in Table 2. Therefore, the two sets of Ω and subsequently the Υ values should also be comparable. However, we notice that Tayal's results for Υ are overestimated by ∼20% in the entire temperature range as shown in Fig. 18. Both of these being allowed transitions converge slowly (see Fig. 2 for example), and therefore a larger range of partial waves as adopted in the present calculations is helpful in a more accurate determination of Ω values. Nevertheless, overall there is no (major) discrepancy between

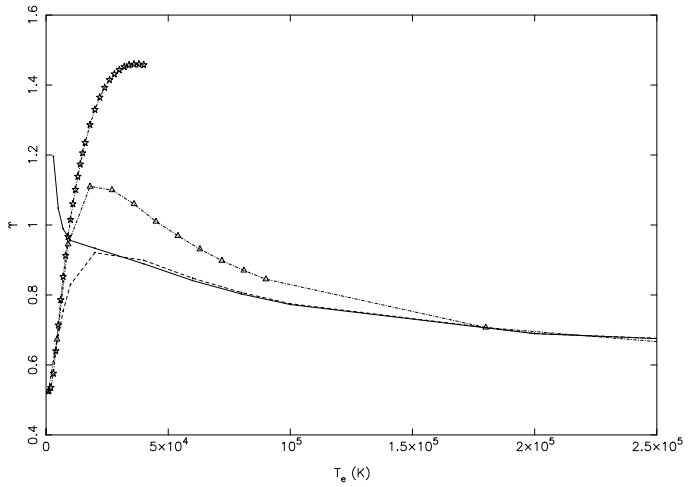

Fig. 16. Comparison of present (continuous curve) effective collision strengths with those of Blum & Pradhan (1992: dot-dash curve with stars), Zhang et al. (1994: dot-dash curve with triangles), and Tayal (2006: broken curve) for the 2−6 ($2s^2 2p\ ^2P^\circ_{3/2}$−$2s2p^2\ ^2D_{3/2}$) transition of O IV.

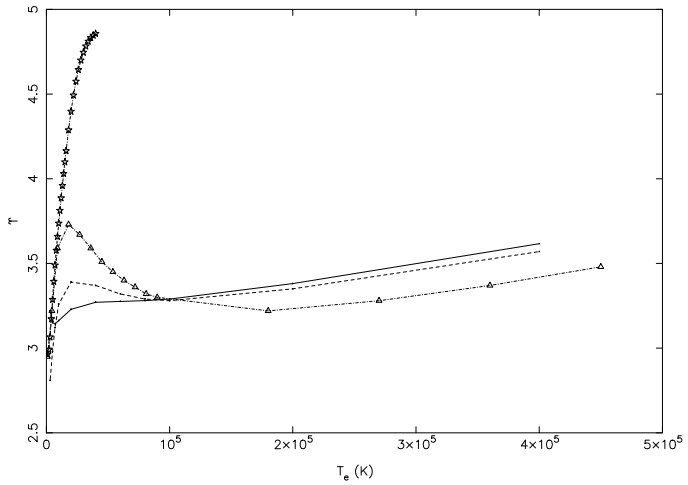

Fig. 17. Comparison of present (continuous curve) effective collision strengths with those of Blum & Pradhan (1992: dot-dash curve with stars), Zhang et al. (1994: dot-dash curve with triangles), and Tayal (2006: broken curve) for the 2−7 ($2s^2 2p\ ^2P^\circ_{3/2}$−$2s2p^2\ ^2D_{5/2}$) transition of O IV.

our calculations and those of Tayal, yet his results are deficient as noted earlier in Sect. 1. We elaborate on these below.

Tayal's (2006) reported data for A- and Υ values are only for a subset of the transitions among the lowest 54 levels of O IV, whereas data for all transitions are required in plasma modelling. Furthermore, his reported values of Υ cannot be applied because of serious printing errors, as the multiplication factors of $10^{\pm n}$ are missing from his Table 4. For transitions such as 1−3, 2−3 and 3−9, if one has a closer look at his results for Υ, corrections of a factor of 100 can be applied as Υ should be lower towards the higher end of the temperature range. However, there are many transitions for which such corrections *cannot* be applied by the users, and examples include: 1−11, 1−12, 1−13, 1−14 and 1−15, because factors of $10^{\pm n}$ are missing in the entire temperature range. This is clearly revealed by a comparison of his results with our values of Υ listed in Table 6. Tayal's results of Υ for these (and many other) transitions are higher by up to three orders of magnitude, because of misprinting.

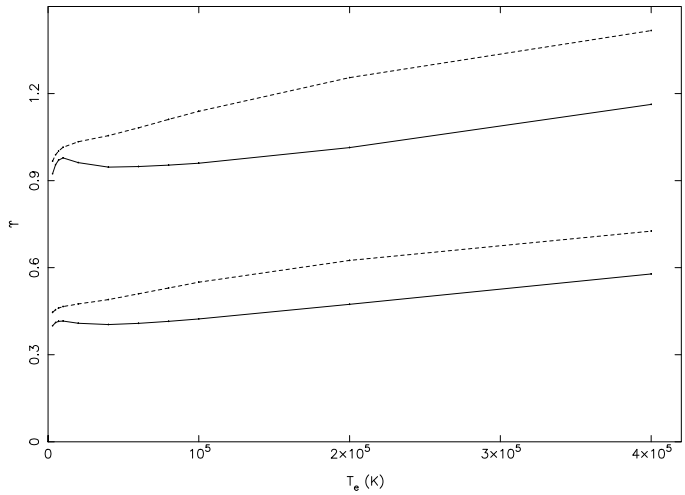

Fig. 18. Comparison of present (continuous curves) effective collision strengths with those of Tayal (2006: broken curves) for the 1−19 ($2s^2 2p\ ^2P^\circ_{1/2}$−$2s^2 3d\ ^2D_{3/2}$, lower curves) and 2−20 ($2s^2 2p\ ^2P^\circ_{3/2}$−$2s^2 3d\ ^2D_{5/2}$, upper curves) transitions of O IV.

7. Conclusions

In this work we have reported energy levels and radiative rates for all transitions among the 75 levels of the $2s^2 2p$, $2s2p^2$, $2p^3$, $2s^2 3\ell$, $2s2p3\ell$, and $2s^2 4\ell$ configurations of O IV. These results have been obtained from the GRASP code, and A-values have been reported for four types of transitions, i.e. E1, E2, M1 and M2. The effect of extensive CI on the accuracy of the listed parameters has been fully assessed. Inclusion of CI with configurations/levels which closely interact improves the accuracy of the wavefunctions, but additional CI with higher lying levels makes an insignificant difference. Our energy levels listed in Table 1b have been assessed to be accurate to better than 3%, while the A-values are accurate to ∼20% for a majority of the strong transitions.

For the scattering work we have adopted the DARC code and have reported excitation rates for all transitions among the above listed 75 levels. Earlier available results of Blum & Pradhan (1992) and Zhang et al. (1994) are limited to a few transitions, and are not assessed to be very accurate. However, there is no major discrepancy with the more recent calculations of Tayal (2006), but his results are available for only a subset of the transitions and are not easy to understand because of printing errors. Furthermore, in the present work the following improvements have been made over his calculations: (i) all 75 levels of the above configurations have been included as opposed to only 54 levels; (ii) the range of partial waves has been increased from the 25 considered by Tayal to 40 in the present work, which results in a better convergence of Ω especially at higher energies; (iii) the energy range over which Ω have been generated has been extended from 20 Ryd to 25 Ryd, which enables us to calculate values of Υ up to $T_e = 10^6$ K, compared to the $T_e \leq 4 \times 10^5$ K of Tayal; and finally (iv) our calculations are in jj coupling which properly accounts for the relativistic effects. Through comparisons made with the earlier results, we assess that the accuracy of our values of Υ is better than 20%. However, due to the presence of near threshold resonances, this accuracy assessment may not be correct for some transitions and for temperatures towards the lower end, particularly when there is scope for improvement in our calculated energy levels as discussed in Sect. 2. Therefore, further improvement over our results can be made by including

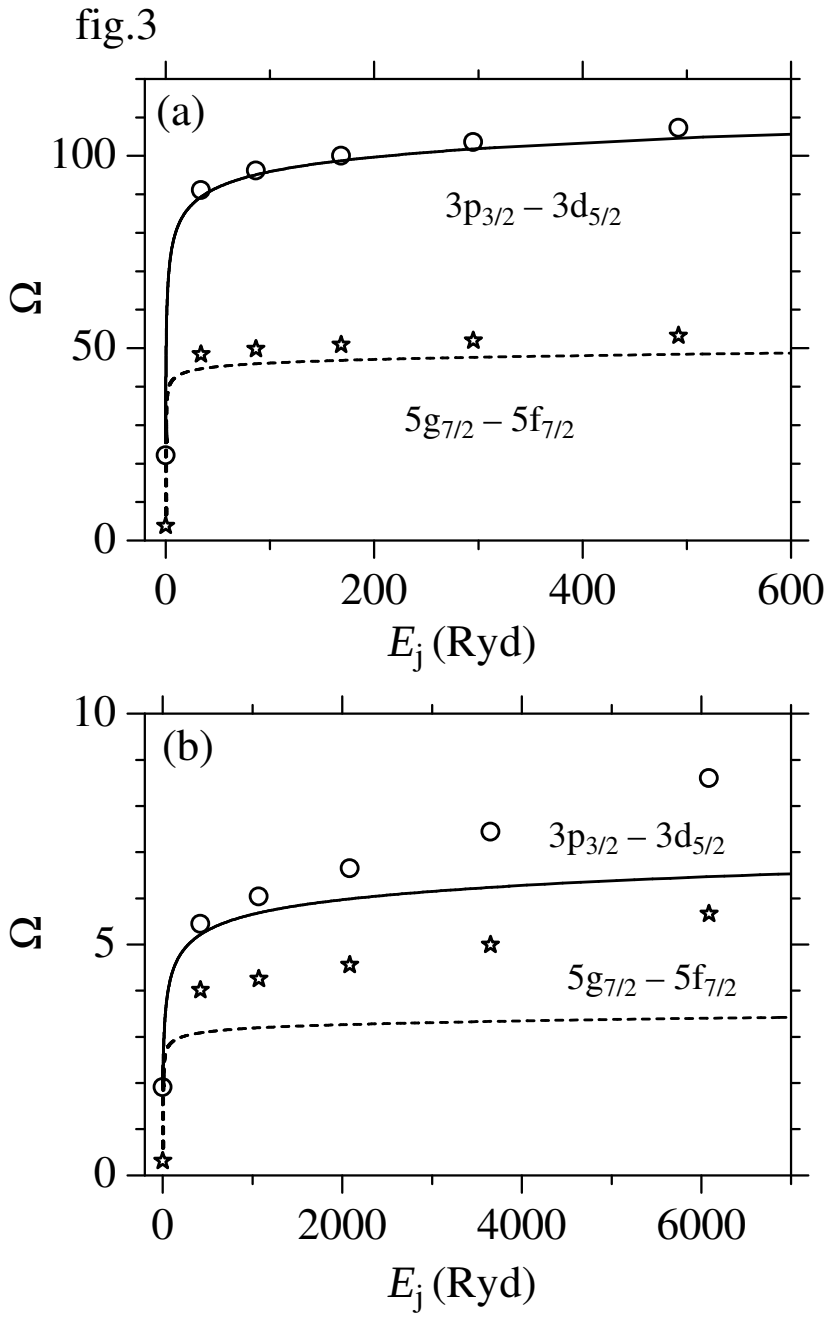

Figure 3: Comparison of collision strengths (Ω) with scattered energy (E_j) for the $3p_{3/2}$ - $3d_{5/2}$ and $5g_{7/2}$ - $5f_{7/2}$ transitions of (a) O VIII and (b) Ni XXVIII. Continuous and broken curves are from CB and circles and stars are from FAC.

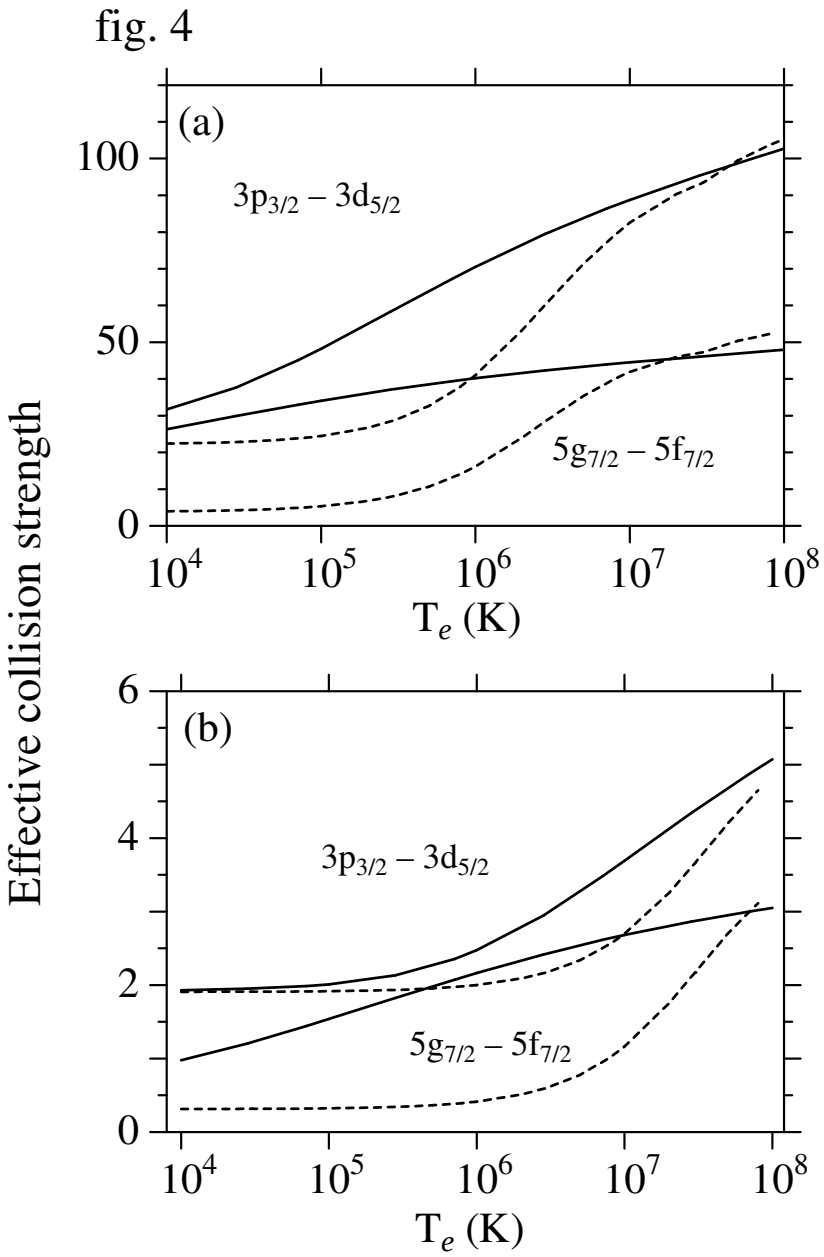

Figure 4: Comparison of effective collision strengths (Υ) for the $3p_{3/2}$ - $3d_{5/2}$ and $5g_{7/2}$ - $5f_{7/2}$ transitions of (a) O VIII and (b) Ni XXVIII. Continuous and broken curves are from CB and FAC, respectively.

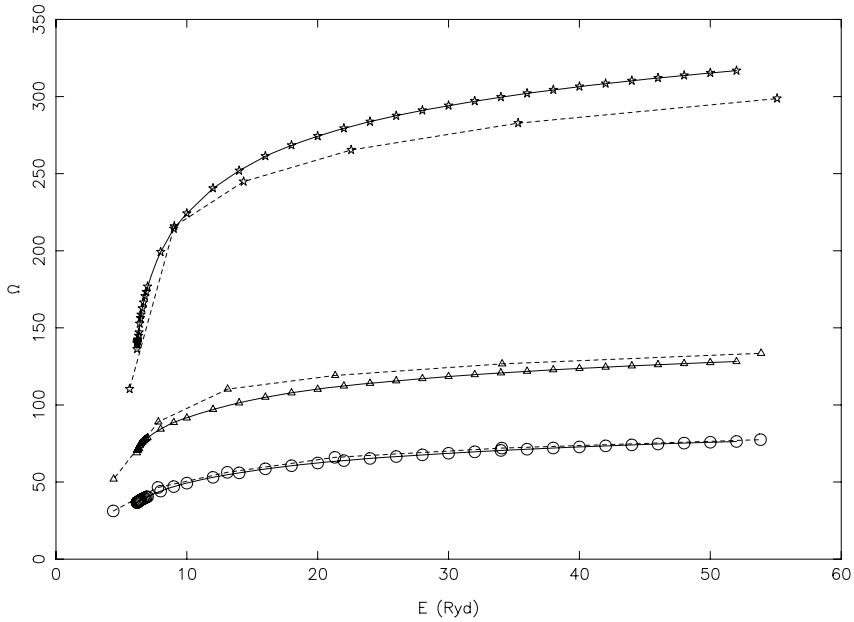

Figure 4. Comparison of collision strengths from our calculations from DARC (continuous curves) and FAC (broken curves) for the 4–6 (circles: 3s $^2S_{1/2}$–3p $^2P^o_{3/2}$), 6–8 (triangles: 3p $^2P^o_{3/2}$–3d $^2D_{5/2}$) and 10–12 (stars: 4p $^2P^o_{1/2}$–4d $^2D_{3/2}$) allowed transitions of N V.

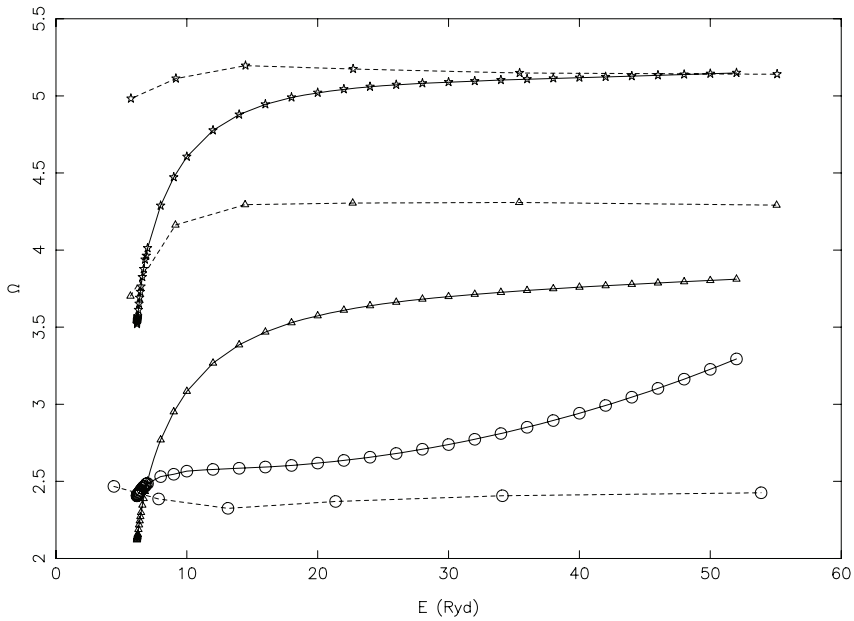

Figure 5. Comparison of collision strengths from our calculations from DARC (continuous curves) and FAC (broken curves) for the 4–8 (circles: 3s $^2S_{1/2}$–3d $^2D_{5/2}$), 6–11 (triangles: 3p $^2P^o_{3/2}$–4p $^2P^o_{3/2}$), and 8–13 (stars: 3d $^2D_{5/2}$–4d $^2D_{5/2}$) forbidden transitions of N V.

can be easily obtained from the following equations:

$$q(i,j) = \frac{8.63\times10^{-6}}{\omega_i T_e^{1/2}}\Upsilon \exp(-E_{ij}/kT_e), \quad \mathrm{cm^3\,s^{-1}} \qquad (8)$$

and

$$q(j,i) = \frac{8.63\times10^{-6}}{\omega_j T_e^{1/2}}\Upsilon, \quad \mathrm{cm^3\,s^{-1}}, \qquad (9)$$

where ω_i and ω_j are the statistical weights of the initial (i) and final (j) states, respectively, and E_{ij} is the transition energy. The contribution of resonances may enhance the values of Υ over those of the background values of collision strengths (Ω_B), especially for the forbidden transitions, by up to a factor of ten (or even more), depending on the transition and/or the temperature. Similarly, values of Ω need to be calculated over a wide energy range (above threshold) in order to obtain convergence of the integral in equation (7), as demonstrated in figure 7 of Aggarwal and Keenan [21].

To delineate resonances, we have performed our calculations of Ω at over 9160 energies in the threshold region. Close to threshold (∼0.1 Ryd above a threshold) the energy mesh is 0.001 Ryd, and away from threshold it is

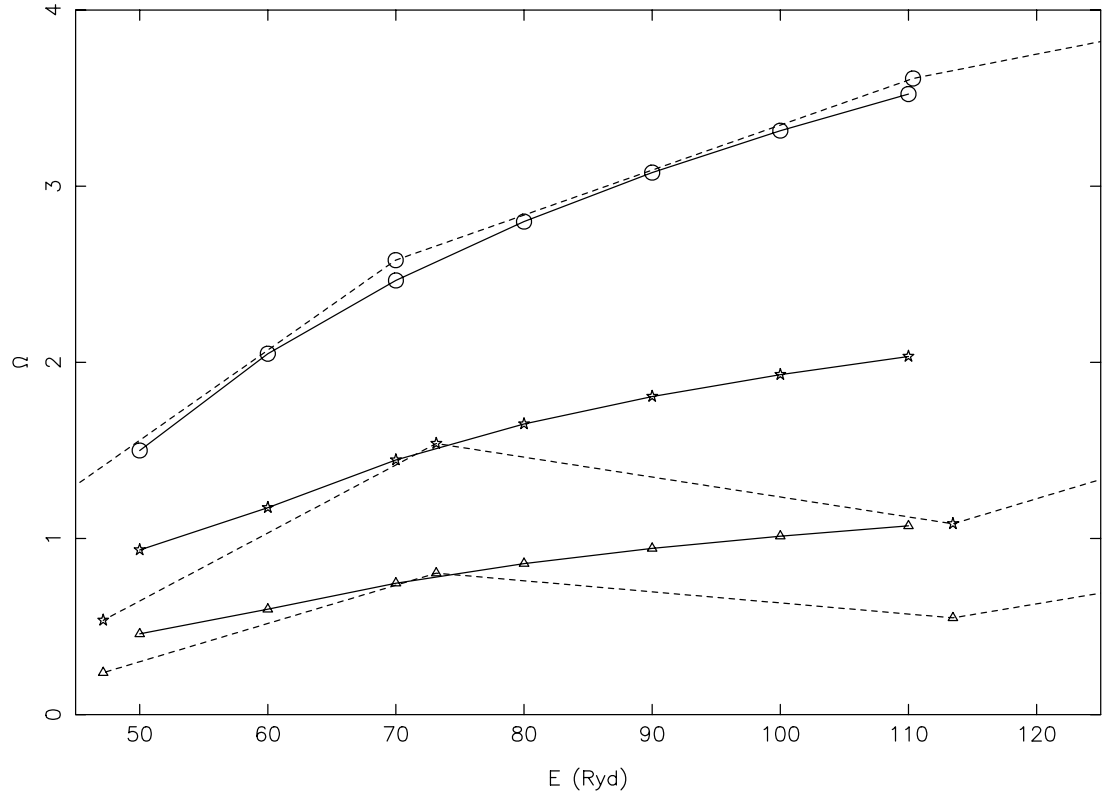

Figure 4. Comparison of collision strengths from our calculations from DARC (continuous curves) and FAC (broken curves) for the 4–9 (circles: $2p\,^2P^o_{3/2}$–$3d\,^2D_{5/2}$), 12–18 (triangles: $4d\,^2D_{3/2}$–$5p\,^2P^o_{1/2}$), and 14–20 (stars: $4d\,^2D_{5/2}$–$5p\,^2P^o_{3/2}$) allowed transitions of N VII.

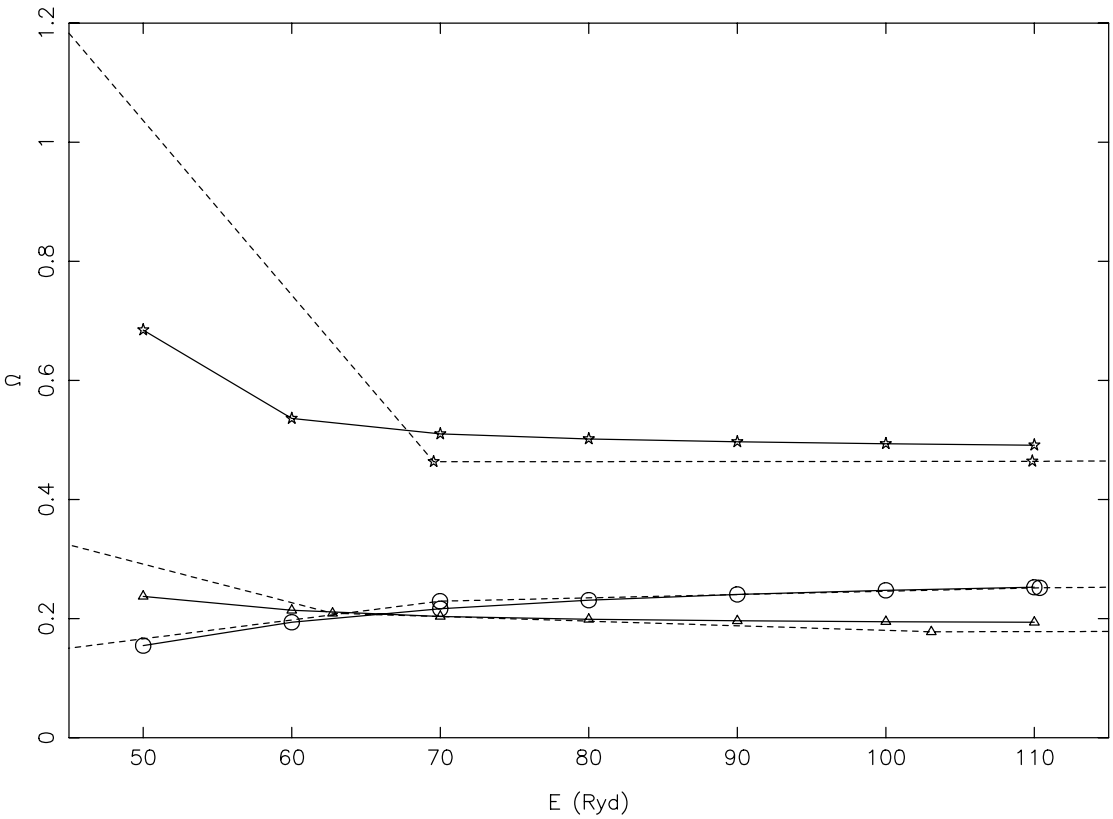

Figure 5. Comparison of collision strengths from our calculations from DARC (continuous curves) and FAC (broken curves) for the 2–7 (circles: $2s\,^2S_{1/2}$–$3d\,^2D_{3/2}$), 3–4 (triangles: $2p\,^2P^o_{1/2}$–$2p\,^2P^o_{3/2}$), and 7–9 (stars: $3d\,^2D_{3/2}$–$3d\,^2D_{5/2}$) forbidden transitions of N VII.

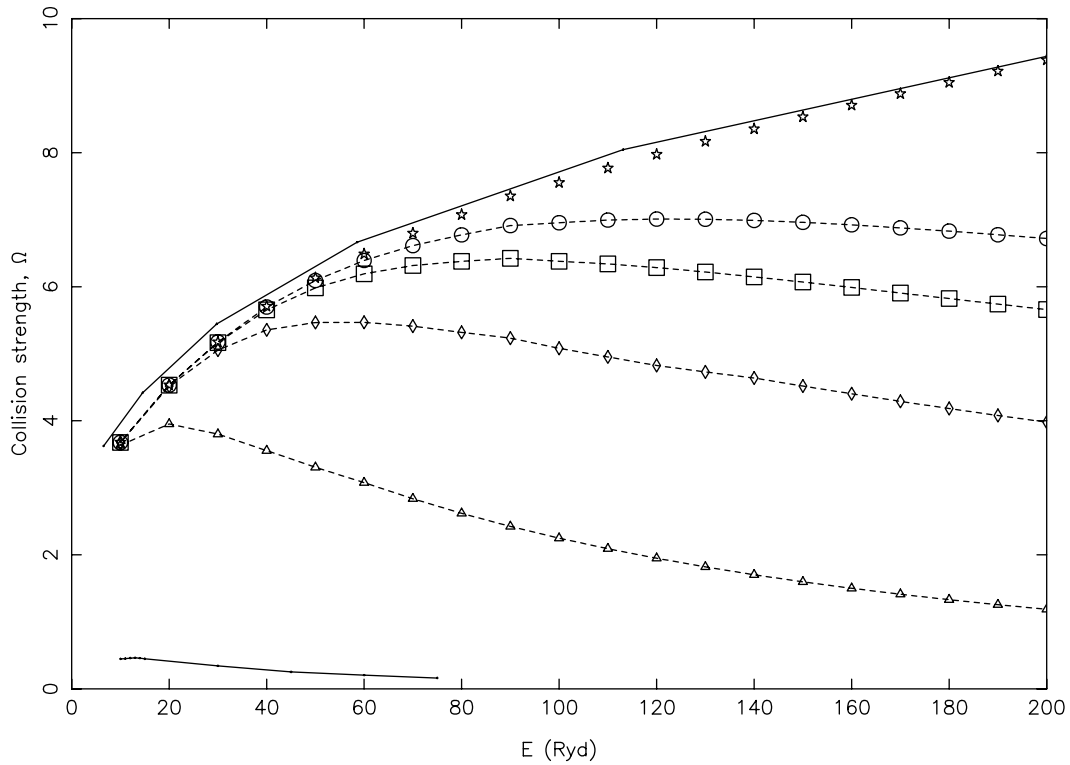

Fig. 2. Comparison of total collision strength (Ω) for the 1–13 ($3s^2 3p^6\ ^1\mathrm{S}_0 - 3s^2 3p^5 3d\ ^1\mathrm{P}^{\mathrm{o}}_1$) transition of Ni XI at energies above thresholds (in Ryd). Lower continuous curve — results of Verma et al. [1], upper continuous curve — present results from FAC, broken curves are our present results from DARC, triangles: $J \leq 9.5$, diamonds: $J \leq 19.5$, squares: $J \leq 29.5$, circles: $J \leq 39.5$, and stars are the converged values with top-up.

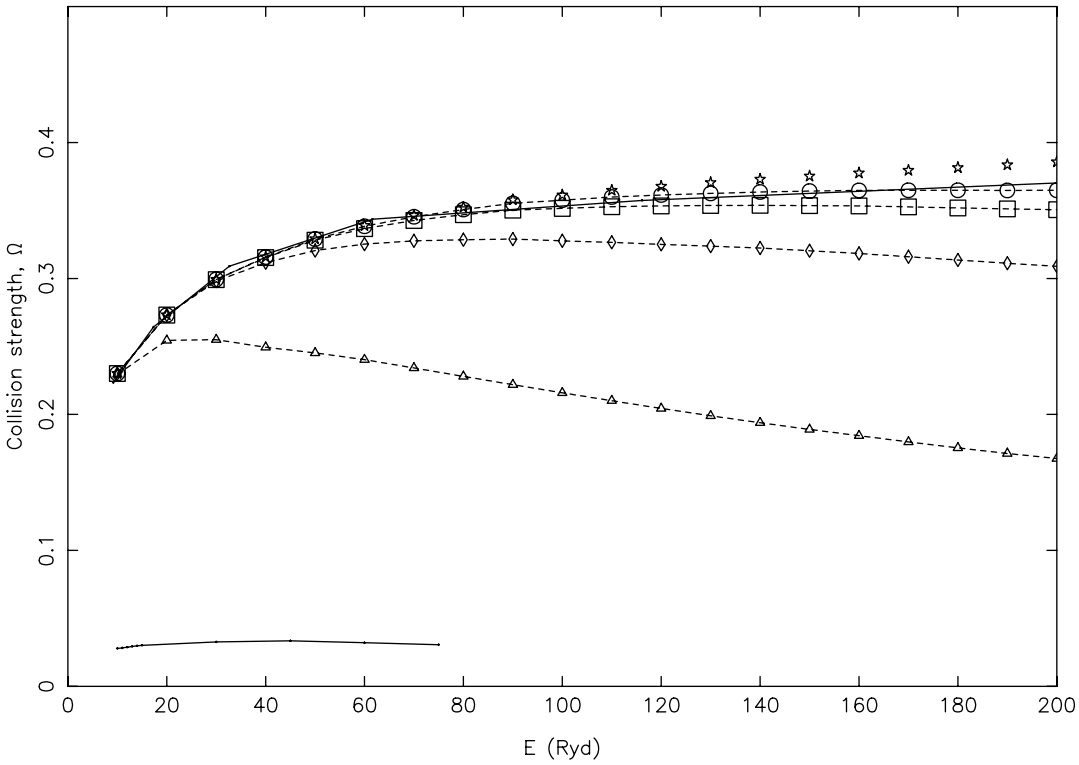

Fig. 3. Comparison of total collision strength (Ω) for the 1–17 ($3s^2 3p^6\ ^1\mathrm{S}_0 - 3s 3p^6 3d\ ^1\mathrm{D}_2$) transition of Ni XI at energies above thresholds (in Ryd). Lower continuous curve — results of Verma et al. [1], upper continuous curve — present results from FAC, broken curves are our present results from DARC, triangles: $J \leq 9.5$, diamonds: $J \leq 19.5$, squares: $J \leq 29.5$, circles: $J \leq 39.5$, and stars are the converged values with top-up.

Table 4. Effective collision strengths for transitions in Ni XI. $a \pm b \equiv a \times 10^{\pm b}$.

Transition		Temperature (10^5 K)										
i	j	1.0	2.0	4.0	6.0	8.0	10.0	20.0	40.0	60.0	80.0	100.0
1	2	3.502−2	2.575−2	1.923−2	1.634−2	1.457−2	1.332−2	9.888−3	6.962−3	5.489−3	4.566−3	3.923−3
1	3	1.249−1	9.247−2	6.812−2	5.696−2	5.017−2	4.546−2	3.310−2	2.332−2	1.862−2	1.573−2	1.371−2
1	4	2.027−1	1.516−1	1.105−1	9.181−2	8.051−2	7.268−2	5.220−2	3.594−2	2.808−2	2.325−2	1.991−2
1	5	1.374−1	1.081−1	8.259−2	6.969−2	6.147−2	5.558−2	3.974−2	2.705−2	2.101−2	1.732−2	1.479−2
1	6	1.934−1	1.388−1	9.666−2	7.760−2	6.630−2	5.865−2	3.998−2	2.708−2	2.152−2	1.825−2	1.603−2
1	7	1.735−1	1.147−1	7.517−2	5.868−2	4.923−2	4.296−2	2.799−2	1.784−2	1.348−2	1.094−2	9.248−3
1	8	1.264−1	1.110−1	8.804−2	7.423−2	6.532−2	5.914−2	4.457−2	3.641−2	3.384−2	3.246−2	3.133−2
1	9	9.752−2	8.484−2	6.644−2	5.434−2	4.615−2	4.027−2	2.537−2	1.532−2	1.123−2	8.941−3	7.462−3
1	10	2.961−2	2.881−2	2.684−2	2.561−2	2.483−2	2.432−2	2.343−2	2.385−2	2.460−2	2.505−2	2.510−2
1	11	6.438−2	6.708−2	5.607−2	4.676−2	4.012−2	3.525−2	2.260−2	1.382−2	1.017−2	8.118−3	6.783−3
1	12	1.598−1	1.504−1	1.223−1	1.041−1	9.225−2	8.411−2	6.540−2	5.592−2	5.347−2	5.222−2	5.100−2
1	13	3.372+0	3.454+0	3.603+0	3.732+0	3.845+0	3.948+0	4.383+0	5.045+0	5.503+0	5.776+0	5.894+0
1	14	1.440−2	1.296−2	1.165−2	1.085−2	1.025−2	9.747−3	7.994−3	6.053−3	4.934−3	4.187−3	3.646−3
1	15	2.409−2	2.176−2	1.965−2	1.837−2	1.738−2	1.655−2	1.365−2	1.042−2	8.567−3	7.324−3	6.421−3
1	16	3.280−2	2.972−2	2.689−2	2.513−2	2.377−2	2.262−2	1.858−2	1.407−2	1.147−2	9.731−3	8.475−3
1	17	2.254−1	2.299−1	2.368−1	2.425−1	2.475−1	2.520−1	2.695−1	2.919−1	3.047−1	3.098−1	3.090−1

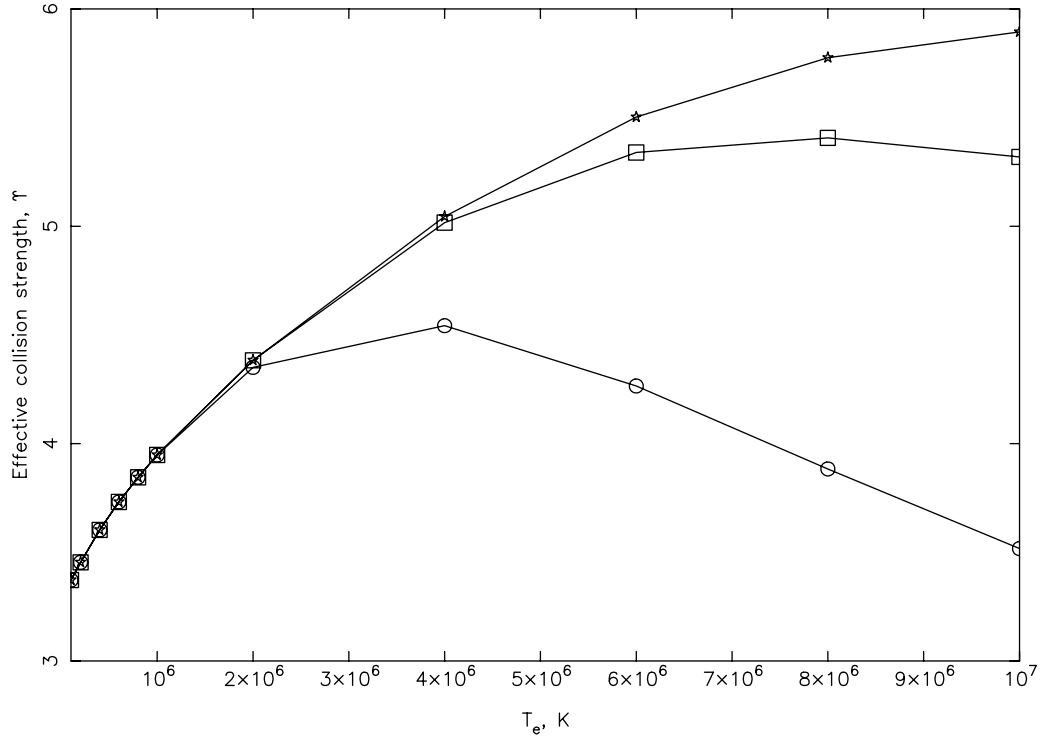

Fig. 7. Effective collision strength (Υ) for the 1–13 ($3s^2 3p^6\ ^1\mathrm{S}_0$ – $3s^2 3p^5 3d\ ^1\mathrm{P}^{\mathrm{o}}_1$) transition of Ni XI. Lower curve (circles) is obtained with $E \leq 75$ Ryd, middle curve (squares) with $E \leq 150$ Ryd, and upper curve (stars) give final converged results.

on the values of Υ, which we will discuss below. Similarly, even for the 1–2 (and other) forbidden transition(s), their Ω values are not only underestimated, but also decrease to almost zero at some energies as shown in their Figure 2, whereas we do not observe any such behaviour. This is again due to the limited range of partial waves adopted by these authors.

In Table 4 we list our values of Υ for all 16 transitions from the ground state to higher excited levels of Ni XI over a wide temperature range of 10^5 to 10^7 K, suitable for applications in astrophysical, fusion and laser-produced plasmas. The only other similar results available in the literature for comparison are those of Verma et al. [1], which are in complete disagreement with ours, because their Ω values are in error. Additionally, further errors are inhibited into their values of Υ, because of the limited range of energy ($E \leq 75$ Ryd) adopted by them. This energy range is *not* sufficient for the convergence of the integral in equation (1) up to the temperature of 10^7 K. To demonstrate the deficiency of their calculations we show our values of Υ for only one transition, namely 1–13 ($3s^2 3p^6\ ^1\mathrm{S}_0$ – $3s^2 3p^5 3d\ ^1\mathrm{P}^{\mathrm{o}}_1$) in Figure 7. The lowest

SOURCES OF DATA

CHIANTI:
http://www.damtp.cam.ac.uk/user/astro/chianti/

ADAS:
http://open.adas.ac.uk/

CFADC:
http://www-cfadc.phy.ornl.gov/

ADVICE

Producers

1. Make as much comparisons as possible for a variety of transitions, such as: allowed, forbidden, semi-forbidden, weak, and strong.
2. In case of large differences, try to understand and explain those without making assumptions.
3. Report results for collision strengths (Ω) at least for a few transitions and at a few energies so that some idea can be obtained about the relationship between Ω and Υ.

Users

1. Situation is the best when only one set of data is available - often not!
2. If two or more data sets are available and authors do not fully and convincingly justify the improvements made, use both of them and make your own assessment, but **remember** that latest calculations may not always be the best.
3. In case of doubt and/or suspicion, contact the authors.

Assessors

1. Difficult when you cannot assess your own work!
2. Assess what methods and assumptions have been used.
3. Follow some basic guidelines, such as: behaviour of a transition, adequacy of the J/L and E ranges, inclusion (exclusion) of resonances, relativistic effects, etc.